

## From the comfort zone to crown dieback: Sequence of physiological stress thresholds in mature European beech trees across progressive drought



Lorenz Walthert<sup>a,\*</sup>, Andrea Ganthaler<sup>b</sup>, Stefan Mayr<sup>b</sup>, Matthias Saurer<sup>a</sup>, Peter Waldner<sup>a</sup>, Marco Walser<sup>a</sup>, Roman Zweifel<sup>a</sup>, Georg von Arx<sup>a</sup>

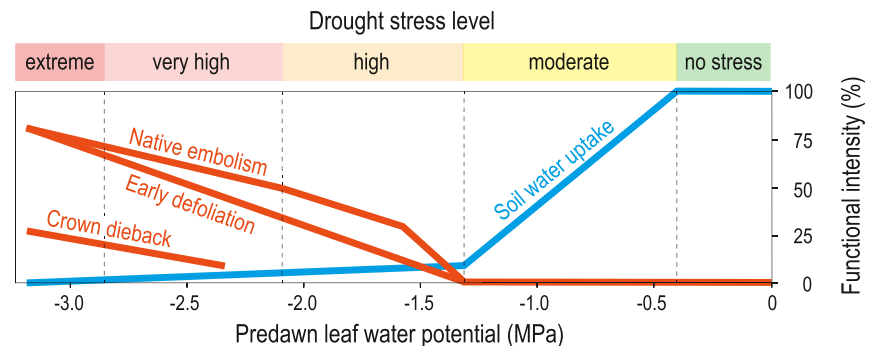
<sup>a</sup> Swiss Federal Institute for Forest, Snow and Landscape Research WSL, Zürcherstrasse 111, 8903 Birmensdorf, Switzerland

<sup>b</sup> Department of Botany, University of Innsbruck, Sternwartestrasse 15, 6020 Innsbruck, Austria

### HIGHLIGHTS

- We studied the hydraulic behaviour of mature *Fagus sylvatica* trees.
- Data from multiple near-natural soil-plant-atmosphere continua (SPAC) were collected.
- The observed physiological drought responses were coherent across sites.
- The results were synthesised into an empirical stress scheme for beech.
- Our study provides relevant and fundamental information for species range predictions.

### GRAPHICAL ABSTRACT



### ARTICLE INFO

#### Article history:

Received 29 June 2020

Received in revised form 14 August 2020

Accepted 17 August 2020

Available online 21 August 2020

Editor: Elena Paoletti

#### Keywords:

Early defoliation

*Fagus sylvatica*

Native embolism

Soil water potential

Soil water uptake

Tree water deficit

### ABSTRACT

Drought responses of mature trees are still poorly understood making it difficult to predict species distributions under a warmer climate. Using mature European beech (*Fagus sylvatica* L.), a widespread and economically important tree species in Europe, we aimed at developing an empirical stress-level scheme to describe its physiological response to drought. We analysed effects of decreasing soil and leaf water potential on soil water uptake, stem radius, native embolism, early defoliation and crown dieback with comprehensive measurements from overall nine hydrologically distinct beech stands across Switzerland, including records from the exceptional 2018 drought and the 2019/2020 post-drought period. Based on the observed responses to decreasing water potential we derived the following five stress levels: I (predawn leaf water potential  $> -0.4$  MPa): no detectable hydraulic limitations; II ( $-0.4$  to  $-1.3$ ): persistent stem shrinkage begins and growth ceases; III ( $-1.3$  to  $-2.1$ ): onset of native embolism and defoliation; IV ( $-2.1$  to  $-2.8$ ): onset of crown dieback; V ( $< -2.8$ ): transpiration ceases and crown dieback is  $>20\%$ . Our scheme provides, for the first time, quantitative thresholds regarding the physiological downregulation of mature European beech trees under drought and therefore synthesises relevant and fundamental information for process-based species distribution models. Moreover, our study revealed that European beech is drought vulnerable, because it still transpires considerably at high levels of embolism and because defoliation occurs rather as a result of embolism than preventing embolism. During the 2018 drought, an exposure to the stress levels III-V of only one month was long enough to trigger

\* Corresponding author.

E-mail address: [lorenz.walthert@wsl.ch](mailto:lorenz.walthert@wsl.ch) (L. Walthert).

substantial crown dieback in beech trees on shallow soils. On deep soils with a high water holding capacity, in contrast, water reserves in deep soil layers prevented drought stress in beech trees. This emphasises the importance to include local data on soil water availability when predicting the future distribution of European beech. © 2020 Elsevier B.V. All rights reserved.

## 1. Introduction

Climate change is leading to more severe and longer drought episodes in many regions worldwide (Dai, 2013; Trenberth et al., 2014) including mountainous environments such as the European Alps (Gobiet et al., 2014; Milano et al., 2015), causing stress responses, reduced productivity, mortality and tree species range shifts in numerous forest biomes (Allen et al., 2010; Williams et al., 2013; Martínez-Vilalta and Lloret, 2016; McDowell et al., 2020). Predictions of future drought-induced forest dynamics and species range shifts require reliable data on temporal and spatial changes of environmental factors, as well as on key ecophysiological processes. The latter determine species competitiveness and mortality under drought, which represent important plant characteristics in vegetation models (Choat et al., 2018; Hartmann et al., 2018). However, the current understanding of the mechanisms involved in drought-related stress behaviour and decline of tree species is limited.

The processes underlying tree survival or death during severe drought are complex (McDowell et al., 2008; Hartmann et al., 2018). Existing conceptual frameworks postulate that tree hydraulics play a key role (Sperry and Love, 2015; Adams et al., 2017; Choat et al., 2018), and in many situations it is considered more important than other factors, such as carbon balance (Choat et al., 2012; Körner, 2015). Within the soil–plant–atmosphere continuum (SPAC), transmission of water potential ( $\Psi$ ), induced by transpiration in the leaves, down to the roots and soil causes a passive flow of water through the tree (Oliveira et al., 2014). During drought, trees control water loss by stomatal regulation, they downregulate their physiological activity, and in many species leaf and branch shedding is a further strategy to mitigate water loss (Tyree et al., 1993; Rood et al., 2000; Wason et al., 2018). Despite these water-saving mechanisms,  $\Psi$  may decrease, leading to the formation of embolisms in the xylem (Tyree and Sperry, 1989; Zweifel and Zeugin, 2008), which disrupt water transport in the tree. Persistent drought may also lead to desiccation of the rooting zone until the permanent wilting point (PWP) is reached and water uptake by roots ceases (Bréda et al., 2006). The concept of hydraulic failure postulates that increasing loss of conductance in the xylem and subsequent deficits in water transport cause tree death. As trees try to avoid embolism formation, xylem vulnerability curves may help to predict mortality thresholds of different species (e.g. Choat et al., 2012; Choat et al., 2018).

Physiological responses to drought other than hydraulic failure can provide additional insights into a species' stress behaviour and performance under drought (Delzon and Cochard, 2014; Bartlett et al., 2016; Choat et al., 2018; McDowell et al., 2019): these drought responses include reductions in soil water uptake by roots (Bunce et al., 1977; Warren et al., 2005) and stomatal adjustments (Bartlett et al., 2016), as observed through measurements of leaf gas exchange, predawn versus midday leaf  $\Psi$  (Aussenac and Granier, 1978; Martínez-Vilalta et al., 2014), and stable isotope ratios in leaf compounds (Bögelein et al., 2012). Further indications of drought stress are an increasing tree water deficit (Zweifel et al., 2005), early defoliation (Tyree et al., 1993) and crown dieback (Cavin et al., 2013). All these drought responses affect tree performance and therefore species distribution through impaired competitiveness.

Particularly for mature trees in native forests, there is still no integrative understanding of the aforementioned drought responses leading to reduced performance, crown dieback or mortality. However, such knowledge is important to provide a basis for more reliable predictions

of species distribution under future climate. This also holds for European beech (*Fagus sylvatica* L.), a common and economically important tree species in Europe. Despite much research on the drought sensitivity of this species, major uncertainties remain. While beech has been shown to be relatively vulnerable to drought in some studies (e.g. Köcher et al., 2009; Scherrer et al., 2011; Weber et al., 2013; Walthert and Meier, 2017; Vanhellefont et al., 2019), others have demonstrated a low vulnerability of this species even under substantial drought (Pflug et al., 2018; Dietrich et al., 2019). These contrasting findings might partly be explained by how drought was defined and quantified, but also by differences in methodology, investigated tree traits and related drought responses. In addition, we emphasise two aspects: first, in ecophysiological drought studies on mature beech trees at forest sites, study trees were not exposed to severe drought stress, as early defoliation and drought-induced damage were absent (e.g. Backes and Leuschner, 2000; Aranda et al., 2005; Leuzinger et al., 2005; Nahm et al., 2007; Fotelli et al., 2009; Scherrer et al., 2011; Sitková et al., 2014; Dietrich et al., 2019; but see Peiffer et al., 2014 and Schuldt et al., 2020). Second, responses of beech trees to more severe drought were mainly examined using juvenile or potted trees under experimental conditions (e.g. Barigah et al., 2013; Urli et al., 2013; Pflug et al., 2018). As juvenile and mature trees differ in physiology (Ryan and Yoder, 1997; Kolb and Matyssek, 2001), findings from potted, juvenile trees may not translate well to drought responses of mature trees growing under natural conditions (Choat et al., 2018). In addition, soils and tree rooting are often neglected or only superficially considered in drought studies although the pedosphere is part of the hydrosphere and therefore has the potential to modify effects of atmospheric drought on plants (Rambal, 1984; Nardini et al., 2016; Phillips et al., 2016). Depending on the storage capacity of plant available soil water (AWC) and the actual soil water reserves, soils can mitigate or even worsen atmospheric drought effects. Currently it is unclear whether water reserves in deep soil layers are extracted by roots of mature beech trees and thus contribute to reduce drought stress.

In the present study, we aimed to shed light on the drought stress behaviour of mature European beech trees under natural stress conditions. To that end, we investigated the hydraulics of beech trees from a network of near-natural beech forest sites over a wide range of water availability conditions. Our study period included the extraordinary 2018 summer drought in Switzerland, when mature beech trees at several of these sites were severely impacted. With data from four spheres – atmosphere, biosphere, hydrosphere and lithosphere – we analysed the effect of decreasing soil and tree  $\Psi$  on soil water uptake, transpiration, tree water deficit, native embolism formation, early defoliation and crown dieback. Our hypotheses were: i) mature beech trees respond coherently to progressive drought at different study sites, making it possible to establish a general scheme for the drought stress behaviour of European beech, ii) the observed physiological responses and stress symptoms allow a stress classification with specific characteristics of plant performance (i.e., stem shrinkage, leaf wilting etc.), and iii) water reserves in deep soil layers mitigate atmospheric drought effects on mature beech trees.

## 2. Material and methods

### 2.1. Study plots

The drought responses of beech trees were investigated in overall nine beech forest plots that differ greatly in their water supply. The

study plots are part of two research platforms from the Swiss Federal Institute for Forest, Snow and Landscape Research WSL, the Forest Soil Database (FSDB) and TreeNet ([www.treenet.info](http://www.treenet.info)), and are scattered across Switzerland (Central Europe, circa 46–48°N and 6–10°E) between 500 and 900 m a.s.l. (Table 1). Averaged over the period 1981–2010, the mean annual air temperature in the plots was between 8.5 and 9.4 °C and the annual precipitation sum was between 815 and 1368 mm (Remund et al., 2014; Table 1). During the vegetation period 2018, many regions of Switzerland experienced one of the most severe droughts since the onset of meteorological records with precipitation deficits exceeding return periods of 70 years (Brunner et al., 2019). From April to September 2018, the study plots were exposed to air temperatures 2.3–2.7 °C higher and precipitation sums 35–55% lower than the respective long-term means from 1981 to 2010, and with precipitation sums in the plots ranging from 265 to 504 mm (MeteoSwiss, 2016a, 2016b; Table 1). During the peak of drought from mid-July to mid-August 2018, daily maximal temperatures were between 30 and 33 °C on nearly every day. In all study plots, tree species composition was near natural, with mean tree age ranging from 66 to 165 years, tree height from 12 to 39 m, and leaf area index from 4.2 to 6.3 (Table 1). Three plots represented mixed beech stands with moderately dense herb or shrub layers, whereas the six remaining plots were covered by nearly pure beech stands with rather sparse herb and shrub layers (Table 1). Depending on the parent material (moraine, loess, limestone, marl and conglomerates), the soils had different depths and AWCs, ranging from 0.8 to >2.0 m and from 80 to >425 mm, respectively (Table 1). Visual assessment did not reveal redoximorphic features in any soil, which indicates that trees did not suffer from oxygen deficits in the rooting zone. The same visual assessment indicated that roots were present in all soils down to the maximal exploration depth.

Relationships between soil water availability and defoliation of beech crowns were analysed in a subset of six long-term monitoring plots with contrasting AWCs: three plots with deep soils (>2 m depth) and high AWCs (D1–D3) and three plots with rather shallow soils (0.8–1.8 m depth; S1–S3; Tables 1, 2). Both, the plots with deep (D1–D3) and shallow soils (S1–S3) are located in different geographic and climatic regions of Switzerland (see map in Fig. 1) – in a dry central Alpine valley (D2 and S1), in the Jura mountains (D3 and S3) and in the hilly and mountainous eastern part of Switzerland (D1 and S2) with more oceanic climate conditions. In the plots D1–D3, tall beech trees with heights of around 30–40 m indicated favourable forest site conditions whereas in the plots S1–S3 moderate tree heights of around 12–20 m and the admixture of drought tolerant tree species were signs of an adverse water availability. In an additional subset of three well distributed pure beech plots with contrasting AWCs (P1–P3; see map in Fig. 1), a comprehensive dataset on physiological drought responses of beech trees was formed (Tables 1, 2). In P1 with a high AWC, long-term time series of physiological parameters were assessed. The plots P2 and P3 with medium AWCs were selected ad hoc during the 2018 drought peak based on their high percentage of strongly defoliated beech trees by the end of July. Moreover, both plots appeared to be suitable for studying plant and soil water relationships due to compact bedrock that clearly defined the range of the rooting zone.

2.2. Forest stand data

The mean age of the forest stands was estimated based on tree rings from wood cores sampled in 2017 (monitoring plots) or 2008 (ad hoc plots P2 and P3) from three dominant trees in each plot. The height of these trees was recorded with a Vertex II (Haglöf, Långsele, Sweden). The leaf area index (LAI) in the monitoring plots was assessed according to Thimonier et al. (2010) using hemispherical photos taken in late summer of 2013–2015 at five points in the forest stand. The LAI of the ad hoc plots P2 and P3 was calculated according to Schleppi et al. (2011) with data from vegetation inventories.

Table 1 Environmental conditions and forest characteristics in the nine study plots.

Plot ID <sup>a</sup>	Plot name	Research infrastructure <sup>b</sup>	Topography		Climate (1981–2010)		Meteorology (04.–09. 2018)		Soil		Vegetation		Cover							
			Lat	Long	Elevation	Exp	Slope	Annual temperature mean	Annual precipitation sum	Temperature mean	Precipitation sum	Vapor pressure deficit	Depth mean	Plant available water	Tree species <sup>c</sup>	Tree age	Tallest trees	Leaf area index	Shrub layer	Herb layer
	'N	'E	m a.s.l.	–	%	°C	mm	°C	mm	kPa	m	mm	y	m	–	–	%	%	%	
D1	Sihlwald	FSDB, TreeNet	47.25	8.56	629	NE	13	8.9	1368	16.5	449	0.55	>2.0	>295	FASY	113	39	6.0	10	1
D2	Chamoson_N	FSDB, TreeNet	46.21	7.21	876	E	65	8.5	870	16.6	311	0.80	>2.0	>230	FASY	74	29	5.5	5	1
D3	Baerschwil_N	FSDB	47.39	7.45	685	NE	42	8.6	1218	16.4	503	0.56	>2.0	>150	FASY	128	34	4.7	20	10
S1	Chamoson_S	FSDB, TreeNet	46.21	7.21	882	SE	90	8.6	815	18.0	311	0.99	1.8	180	FASY, QUPE, PISY	66	12	4.5	40	2
S2	Tamins	FSDB	46.83	9.42	656	SE	50	9.1	1114	18.3	305	0.88	0.8	110	FASY, QUPE, SOAR	151	12	4.4	70	20
S3	Baerschwil_S	FSDB	47.39	7.46	693	SE	55	8.8	1208	17.6	504	0.79	0.8	80	FASY, QUPE, SOAR	155	19	5.5	30	30
P1	Saillon	FSDB, TreeNet	46.17	7.17	889	SE	55	9.4	829	17.5	265	0.88	>2.0	>425	FREX	100	23	6.3	5	2
P2	Mels	FSDB	47.07	9.39	495	NE	35	9.3	1254	na	340	na	0.8	200	FASY	165	15	4.2	10	25
P3	Reiden	FSDB	47.23	7.98	555	SE	30	9.1	1154	na	453	na	1.0	180	FASY	118	26	4.5	20	1

<sup>a</sup> Study plots on deep (D1–D3) or shallow (S1–S3) soils; study plots with comprehensive physiological measurements (P1–P3).

<sup>b</sup> Forest soil database at the research institute WSL (FSDB).

<sup>c</sup> *Fagus sylvatica* (FASY), *Quercus pubescens* (QUPE), *Quercus petraea* (QUPE), *Fraxinus excelsior* (FREX), *Sorbus aria* (SOAR), *Pinus sylvestris* (PISY).

**Table 2**  
Measurement parameters, intervals and dates for the nine study plots.

Plot ID	Plot type <sup>a</sup>	Start of monitoring	Air temperature	Relative humidity	soil water potential	Stem radius	Leaf water potential	13C/12C isotope ratio	Native embolism	Xylem vulnerability	Early defoliation	Crown dieback
			°C	%	MPa	µm	MPa		%	%	%	%
D1	M	2013	Hourly	Hourly	Hourly	10 min	–	–	–	–	15.-30.09.18	–
D2	M	2013	Hourly	Hourly	Hourly	10 min	–	–	–	–	15.-30.09.18	–
D3	M	2013	Hourly	Hourly	Hourly	–	–	–	–	–	15.-30.09.18	–
S1	M	2014	Hourly	Hourly	Hourly	10 min	–	–	–	–	15.-30.09.18	–
S2	M	2013	Hourly	Hourly	Hourly	–	–	–	–	–	15.-30.09.18	–
S3	M	2013	Hourly	Hourly	Hourly	–	–	–	–	–	15.-30.09.18	–
P1	M	2013	Hourly	Hourly	Hourly	10 min	Occasionally	Occasionally	20/09/2018	20/09/2018	15.-30.09.18	06/2019, 06/2020
P2	AD	–	–	–	01/08/18	–	01/08/18	01/08/18	22/08/18	–	15.-30.09.18	06/2019, 06/2020
P3	AD	–	–	–	12/08/18	–	12/08/18	12/08/18	22/08/18	–	15.-30.09.18	06/2019, 06/2020

<sup>a</sup> Long-term monitoring plot (M); ad hoc 2018 drought plot (AD).

### 2.3. Weather and climate data

Air temperature and relative humidity have been measured in all seven monitoring plots since 2013 at hourly intervals (Table 2) with EL-USB-2+ data loggers (Lascar Electronics Ltd., Salisbury, UK). In each plot three loggers are mounted on different trees at 2 m height.

Hourly values are reported as the mean value of three loggers whereat outliers due to insolation of loggers were excluded from the calculation of the mean. Vapor pressure deficit (VPD) was calculated from temperature and relative humidity. Weather data from the meteorological network of MeteoSwiss were used to derive climate data for the period 1981–2010 (Remund et al., 2014) and to calculate anomalies of air

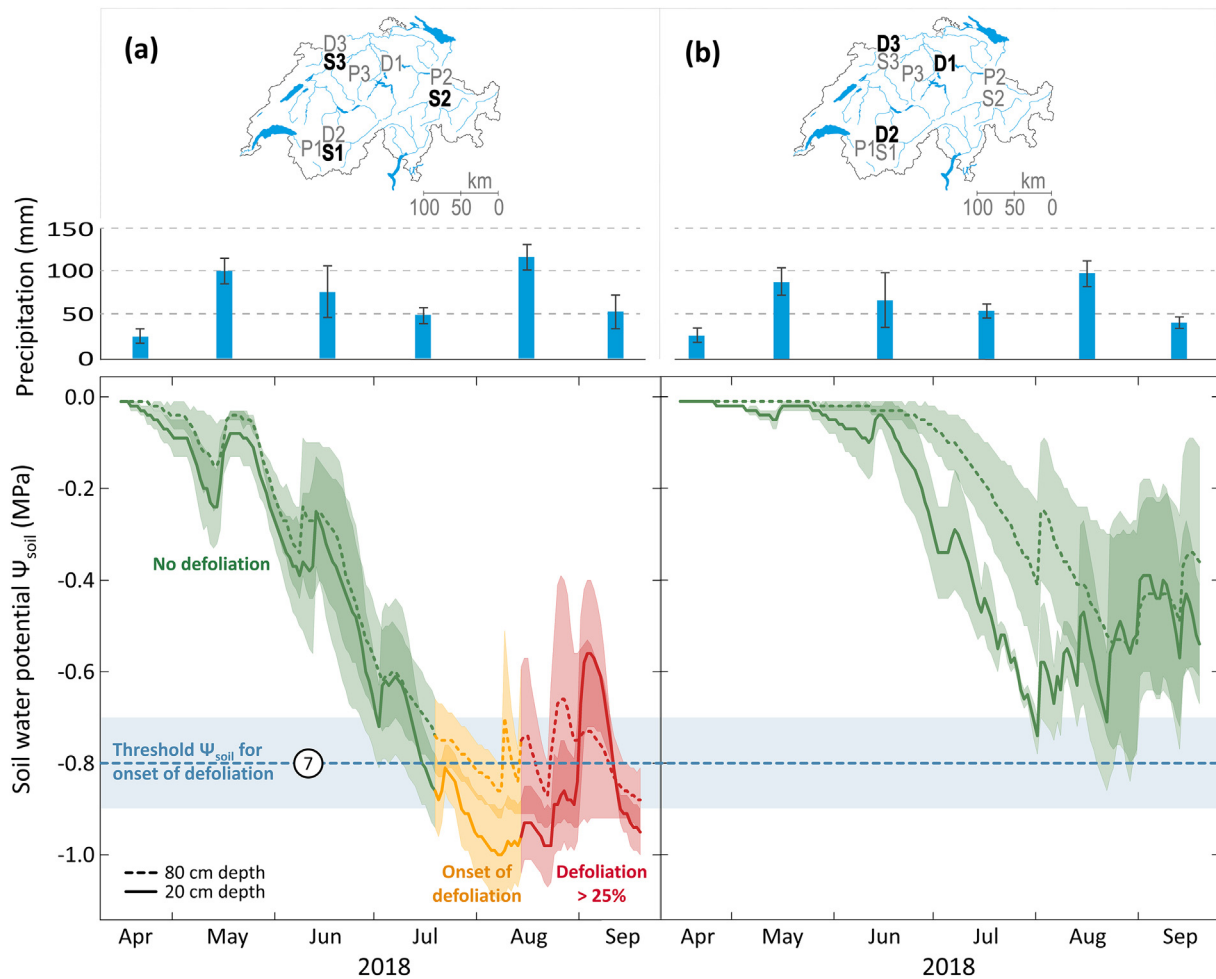


**Fig. 1.** Precipitation, soil water potential ( $\Psi_{\text{soil}}$ ) and defoliation of beech trees (*F. sylvatica*) during the drought year 2018. Pooled monthly precipitation sums (mean  $\pm$  1 SE) and pooled  $\Psi_{\text{soil}}$  at 20 and 80 cm depth (mean  $\pm$  1 SE) are shown for a) three mixed beech-oak stands with early defoliation on shallow soils (plots S1–S3) and b) three beech stands without early defoliation on deep soils with high water storage capacities (plots D1–D3). The point ⑦, onset of defoliation, is used in the synthesis (Fig. 7).



temperature and precipitation as well as precipitation sums for the drought period April to September 2018 (MeteoSwiss, 2016a, 2016b).

#### 2.4. Soil water data

$\Psi_{\text{soil}}$  and soil temperature have been recorded at all seven long-term monitoring plots since 2013 at hourly intervals (Table 2) with MPS-2 sensors and EM-50 data loggers (Decagon Devices, Pullman, WA, USA). For sensor installation, a soil profile was excavated in the centre of a group of dominant trees in each study plot. Two to three MPS-2 sensors were embedded in the front wall of the soil pit at 20 and 80 cm depth in all plots, and additional sensors were installed at 140 and 180–200 cm depth in four plots (D1, D2, S1 and P1). For the plots with rather shallow soils (S1–S3), the sensors span the whole soil depth down to the bedrock.  $\Psi_{\text{soil}}$  measurements were temperature corrected to 22 °C according to Walthert and Schleppei (2018). In the plots P2 and P3 that we selected ad hoc at the peak of the 2018 drought,  $\Psi_{\text{soil}}$  was measured with a Dew Point Potentiometer WP4C (METER Group, Pullman, WA, USA) in soil samples extracted with an Edelman soil auger (Eijkelkamp, Giesbeek, the Netherlands) from locations close to three selected dominant beech trees per plot (study trees). Around each tree, six boreholes were drilled in three directions (0°, 120° and 240°) at a distance of 2.5 and 5 m from the stem. Sampling depths were 0–10, 40–60 and, where possible, 90–110 and 140–160 cm, with the deepest soil sample from each borehole taken directly above the bedrock. Samples (100 samples in total, each ca. 400 g) were immediately packed in plastic bags and stored at 3 °C until measurements of  $\Psi_{\text{soil}}$ .

Because volumetric soil water content was not assessed in the soil profiles, we had to derive water content related parameters by other means. The storage capacity of plant available soil water (AWC) between a soil water potential ( $\Psi_{\text{soil}}$ ) of  $-6$  and  $-1585$  kPa was estimated for all study plots with a pedotransfer function (PTF, Teepe et al., 2003) using data from a soil profile from each plot. Input variables for the PTF were field estimates of soil depth and stone content, as well as measured values of soil density, particle size distribution and humus content, as described by Walthert and Schleppei (2018). For plot P1, daily decreases in volumetric soil water content ( $\theta$ ) were used as a measure for soil water uptake by roots, assuming that soil water flow was negligible (Bréda et al., 1995; Warren et al., 2005). Therefore, the  $\Psi_{\text{soil}}$  measurements were converted into  $\theta$  using a water retention curve for the topsoil and deep soil of P1. The data pairs ( $\Psi$ ,  $\theta$ ) required to establish these curves were taken from Walthert and Schleppei (2018), and the curve fitting to these data pairs was done with RETC (van Genuchten et al., 1991).

#### 2.5. Stem radius changes and tree water deficit

In plots D1, D2, S1 and P1, stem radius changes have been recorded since 2014 at 10-min resolution using automated high-precision point dendrometers (ZN11-T-WP, Natkon, Oetwil am See, Switzerland). In each plot, the two to four dominant beech trees nearest to the MPS-2  $\Psi_{\text{soil}}$  sensors (called study trees hereafter) were equipped with a dendrometer mounted to the stem at a height of about 1.3 m. Tree water deficit (TWD), defined as the difference between a current stem radius value and the preceding maximum, was calculated from the stem radius data according to Zweifel et al. (2016). As TWD expresses a current outer stem tissue water content relative to a fully hydrated condition, it can be used as a continuous measure of tree water status (Zweifel et al., 2005; Drew et al., 2011; Dietrich et al., 2018).

#### 2.6. Leaf water potential

In the plots P1–P3, leaf water potential ( $\Psi_{\text{leaf}}$ ) was measured with a Scholander-type pressure chamber (Model 1000, PMS Instruments, Albany, OR, USA). In P1, measurements were conducted on five sunny days during the vegetation periods 2017 and 2018, every 2–3 h from

04:00 to 17:30. During each recording, three leaves from each of the two study trees were cut from branches near the stem in the lower crown at a height of 2–10 m (as close as possible to the dendrometers), and their  $\Psi_{\text{leaf}}$  was then immediately measured with the pressure chamber. The leaves were then packed in paper bags, dried at 40 °C until constant weight and stored until  $\delta^{13}\text{C}$  analysis was performed (see below). In P2 and P3,  $\Psi_{\text{leaf\_pd}}$  and midday  $\Psi_{\text{leaf\_md}}$  were measured on the same day and by considering the same three study trees as for the survey of  $\Psi_{\text{soil}}$ . The leaf sampling and measurement procedures were identical to those used for P1.

Except at predawn, all sampled leaves were sealed in PMS-bags for 15–30 min prior to abscission. The  $\Psi$  from sealed (not transpiring) leaves can be used as a proxy for stem water potential (McCutchan and Shackel, 1992; Lemoine et al., 2002; Nardini et al., 2013). A bagging time of about 10 min has been shown to be sufficient to reach equilibration between  $\Psi_{\text{leaf}}$  and  $\Psi_{\text{shoot}}$  in deciduous tree species (Fulton et al., 2001).

According to Aussenac and Granier (1978) and Carrière et al. (2020) the difference between daily values of  $\Psi_{\text{leaf\_md}}$  and  $\Psi_{\text{leaf\_pd}}$  measured on sunny days can be used as an indicator for leaf gas exchange, i.e. stomatal and cuticular transpiration, where cessation of gas exchange would occur when this difference is nil (Martinez-Vilalta et al., 2014).

#### 2.7. $\delta^{13}\text{C}$ in water soluble leaf compounds

For isotope analysis, leaves available from the  $\Psi_{\text{leaf\_pd}}$  determination during the field campaigns were used (plots P1–P3). Three leaves per beech tree were re-dried at 65 °C, combined and ground to a fine powder with a MM400 mill (Retsch, Haan, Germany) with zirconginding tools. Water soluble compounds (WSC) were extracted from 60 mg of finely ground leaf material. The samples and 1.5 mL deionised water were put into 2 mL reaction vials and heated in a water bath at 85 °C for 30 min. Subsequently, samples were centrifuged (2 min, 10,000 g) and the supernatant, with the WSC, was transferred to a new reaction vial and stored at  $-20$  °C (Lehmann et al., 2017). Aliquots of 150  $\mu\text{L}$  of the WSC solution, representing ca. 0.1–0.3 mg of carbon, were put into tin capsules (Säntis Analytical, Teufen, Switzerland) and freeze-dried. The samples were then combusted with an excess of oxygen at 1020 °C in an elemental analyser (EA-1110; Carlo Erba, Milan, Italy) and the resulting  $\text{CO}_2$  led to a Delta Plus XL isotope ratio mass spectrometer via a Conflo II interface (both from Thermo Finnigan, Bremen, Germany). All isotope ratios are given in reference to the international standard VPDB in the delta notation in ‰ as  $\delta^{13}\text{C}_{\text{sample}} = (^{13}\text{C}/^{12}\text{C}_{\text{sample}}/^{13}\text{C}/^{12}\text{C}_{\text{standard}} - 1) * 1000$ . Analytical precision was estimated, as the standard deviation of laboratory standards, to be better than 0.2‰.

$\delta^{13}\text{C}$  was used as a short-term integral for water deficit (Peuke et al., 2006), i.e. as a proxy for leaf gas exchange (Bögelein et al., 2012; Pflug et al., 2018) and transpiration. This is based on known isotope fractionations during  $\text{CO}_2$  uptake, which are strongly driven by diffusive limitation, or more precisely by the ratio of photosynthesis to stomatal conductance (Farquhar et al., 1989). The postulated link between  $\delta^{13}\text{C}$  and transpiration is not expected to suffer from non-stomatal limitations to photosynthesis because substantial damage to the photochemical apparatus occurs not before extreme dehydration after full stomatal closure (Trueba et al., 2019).

#### 2.8. Native embolism

In the plots P1–P3, branches of 70–100 cm length and 4–7 mm diameter at their base were collected in the lower crown of five beech trees per plot during the peak of the 2018 drought (Table 2). In P1, branches were cut from the two study trees and from three additional, adjacent beech trees for which we also measured  $\Psi_{\text{leaf}}$  on that day. In P2 and P3, the sampling was 10–20 days after the survey of  $\Psi_{\text{leaf}}$  from the same three study trees per plot as the  $\Psi_{\text{leaf}}$  survey and from two additional dominant beech trees per plot. In P3,  $\Psi_{\text{leaf}}$  at this time was similar to values measured 10 days earlier, while in P2, a rain event

occurred one day before the sampling. However, effects of this rainfall on native embolism were considered negligible, as it was previously reported that beech cannot reverse embolism during periods of rain (Hacke and Sauter, 1995). After branches were cut from the trees, they were wrapped tightly in plastic bags containing moist paper towels and stored at 4 °C until the measurements, which were performed within one week. Branches were re-cut several times under water with a sharp carving knife, removing at least 20 cm in total, to gradually release tension (Wheeler et al., 2013; Beikircher and Mayr, 2016), until a final length of about 30 cm was reached. In addition, all side twigs and the bark at the basal end were removed. Branch segments were then connected to a modified Sperry apparatus (Sperry et al., 1988; Losso et al., 2018) and perfused with distilled, filtered (0.22 µm) and degassed water with 10 mM KCl and 1 mM CaCO<sub>3</sub>, as well as 0.005% (v/v) Micropur (Katadyn Products, Wallisellen, Switzerland) to prevent microbial growth. The initial hydraulic conductance ( $k_i$ ) was measured at 4 kPa before samples were flushed for 20 min at 100 kPa to remove embolisms (Sperry et al., 1988; Beikircher and Mayr, 2016). After flushing, the hydraulic conductance was measured again (final hydraulic conductance;  $k_f$ ). Flushing was repeated up to five times until measurements showed no further increase in conductance. Conductance values were corrected for water viscosity at 20 °C and percent loss of conductance (PLC) was calculated as:

$$\text{PLC} = \left(1 - \frac{k_i}{k_f}\right) * 100$$

### 2.9. Vulnerability to xylem cavitation

Vulnerability to xylem cavitation was assessed with the Cavitrone technique (Cochard et al., 2005) in the five sampled trees from plot P1, taking one branch per tree previously used for native embolism measurements (thus repeatedly flushed and with all native embolisms removed). The measurement procedure followed that of Beikircher et al. (2010). In short, after a final trimming at both ends, samples were fixed in a 280 mm custom-built rotor inside a centrifuge (Sorvall RC-5, Thermo Fisher Scientific, Waltham, MA, USA) and segment ends were kept inside transparent plastic reservoirs filled with water. At successively higher  $\Psi$  values, induced by increasing rotational speed, hydraulic conductance ( $k$ ) through the sample was determined and the percentage loss of conductance (PLC) was calculated based on the initial (maximum) hydraulic conductance (obtained at a xylem pressure of 0.5 MPa) and the hydraulic conductance at a given  $\Psi$ . Curves were fitted with a Weibull regression curve and the threshold value  $\Psi_{50}$ , which refers to  $\Psi$  at 50% PLC, was extracted.

### 2.10. Drought-induced early defoliation

Early defoliation was recorded for all study plots through a visual crown condition assessment in the second half of September 2018. Specifically, crown transparency was estimated in classes of 5% according to images from the Swiss Sanasilva forest inventory (Müller and Stierlin, 1990). In the plots P1–P3, defoliation was estimated for each of the five beech trees per plot that we sampled for native embolism survey. In all other plots, defoliation was assessed as an average of all dominant beech trees growing within a radius of about 25 m around the MPS-2  $\Psi_{\text{soil}}$  sensors. In S1–S3, the dates when beech trees started to defoliate and when they reached a substantial defoliation percentage of about 25% were recorded as well.

### 2.11. Crown dieback

The percentage of crown dieback, i.e. of branches that had recently died, was estimated in plots P1–P3 during the second week of June 2019. In June 2020, the crowns were checked again to assess recovery

or further decline. The visual assessment included the five trees per plot for which native embolism was recorded in 2018.

### 2.12. Statistical analysis

Statistical analyses were performed in R version 3.6 (R Core Team, 2019). The relationship between soil water variables, tree physiological variables and forest stand data were determined using regression analyses. Up to fourth-order polynomial regressions were performed and reduced to third-, second- or first-order polynomial regressions if the quartic, cubic or quadratic terms were not significant. The regression lines were fitted without any theoretical claim as they should merely facilitate the visualisation of trends. The R package “fit-PLC” (Duursma and Choat, 2017) was used for Weibull regression curve fitting to determine vulnerability to xylem cavitation. In all regression plots, significant regression curves ( $P \leq 0.05$ ) and, if not otherwise specified, 95% confidence envelopes are given.

## 3. Results

### 3.1. Soil water dynamics during the 2018 drought

The meteorological drought 2018 was exceptional, both in many regions of Switzerland and at our study plots (see Section 2.1). However, soil water availability varied greatly among the plots as demonstrated by our two groups of contrasting forest sites, three plots (S1–S3) on south-facing slopes with shallow soils of 0.8–1.8 m depth and three north-facing plots (D1–D3) with soils considerably deeper than 2 m (Table 1). Both groups had similar sums and distributions of precipitation from April to September (Fig. 1), however, temperature and VPD were slightly higher in the south-facing forest stands (Table 1).

In April 2018, when the meteorological drought started,  $\Psi_{\text{soil}}$  was around  $-0.01$  MPa and thus near field capacity in all six soils and at all soil depths (Fig. 1a,b) meaning that the precipitation of the winter 2017/2018 saturated the soils to their respective AWC. By the end of May, the shallow soils started to dry out rapidly and showed very low  $\Psi_{\text{soil}}$  values of around  $-0.8$  MPa from July onwards (Fig. 1a). Contrary to the shallow soils, soil drying started one month later in the deep soils and was less severe and more superficial (Fig. 1b). By the end of September,  $\Psi_{\text{soil}}$  in 200 cm depth was still as high as  $-0.1$  MPa in the plot D1 and  $-0.4$  MPa in the plot D2 (data not shown), indicating that there was still relatively easily available soil water in the deep rooting zone. The time series of soil water potential during the summer 2018 additionally reveal that precipitation did not infiltrate deeply into the soils (Fig. 1a,b) and therefore soil water reserves were used. Even though these water reserves amounted to the AWC of the soils in April they were too small to prevent strong soil drying in the shallow soils. In the deep soils with a high AWC, in contrast, the reserves were big enough to inhibit low  $\Psi_{\text{soil}}$ , particularly in deep soil layers.

### 3.2. Early defoliation in 2018

On shallow soils (S1–S3) with a low AWC, early defoliation, i.e. a loss of dry and/or green leaves  $>5\%$ , started around mid-July to mid-August and thus after the meteorological heat and drought had persisted for about 3.5–4.5 months. Defoliation set in when  $\Psi_{\text{soil}}$  in the entire rooting zone decreased to values of about  $-0.8$  MPa (Fig. 1a). In contrast, beech trees on deep soils (D1–D3) with a high AWC, which dried out to a lesser extent, did not show early defoliation (Fig. 1b). Owing to shallow soil wetting from small rain events in late summer, some of the withered herb and shrub species (e.g. *Vaccinium myrtillus*) sprouted again, which was not the case for the defoliated beech trees.

### 3.3. Soil water uptake and tree water status

During rainless periods, there was a clear relationship between the TWD of beech trees (Fig. 2a) and the daily decrease in  $\theta$  (Fig. 2b), which were used as proxies for tree water status and soil water uptake, respectively. Daily water uptake from all soil depths of plot P1 was maximal under moist soil conditions when  $\Psi_{\text{soil}}$  was  $> -0.2$  MPa (Fig. 2b) and the stems were fully hydrated so that TWD was zero (Fig. 2a). Below  $\Psi_{\text{soil}} -0.2$  MPa, soil water uptake decreased and TWD increased with progressive drought (Fig. 2a,b). Between  $\Psi_{\text{soil}} -0.2$  and  $-0.8$  MPa, soil water uptake decreased by 97% on average at all soil depths.

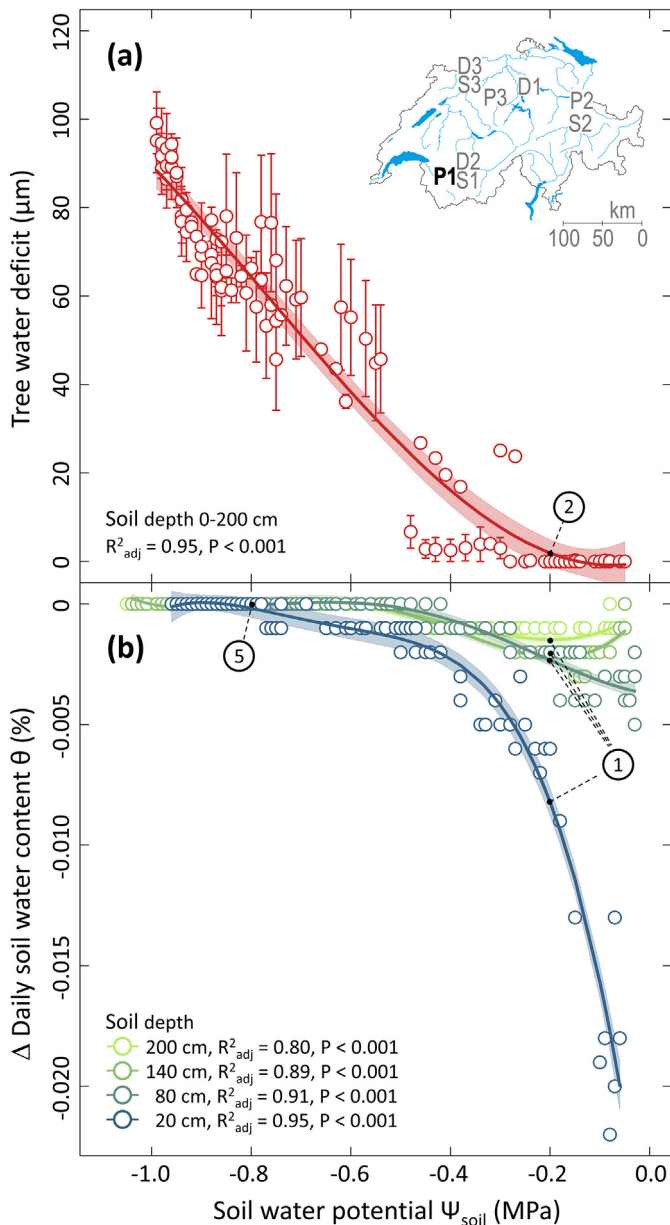


**Fig. 2.** (a) Tree water deficit (TWD) at 06:00 (third-order polynomial regression) and (b) daily decrease in soil water content ( $\theta$ ; a proxy for soil water uptake) between 06:00 and 17:00 (fourth-order polynomial regressions) at four soil depths, both in relation to soil water potential ( $\Psi_{\text{soil}}$ ) at 06:00. All data refer to around 100 days of rainless periods from May to September between 2014 and 2017 in plot P1, where  $\Psi_{\text{soil}}$  in all soil depths decreased to around  $-0.8$  MPa in every summer, paralleled by respective increases of TWD to around  $80 \mu\text{m}$ . Both  $\theta$  and  $\Psi_{\text{soil}}$  represent the mean of several sensors at each soil depth, and TWD represents the mean ( $\pm 1$  SE) of two beech trees (*F. sylvatica*). The points ①, onset of reduced soil water uptake, ②, onset of tree water deficit and ⑤, 97% reduction of soil water uptake, are used in the synthesis (Fig. 7).

In study plots where topsoil and deep soil layers desiccated simultaneously (e.g. plots P1 and S1) the correlation between  $\Psi_{\text{soil}}$  and TWD was very high ( $R^2 = 0.95$  in P1, Fig. 2a;  $R^2 = 0.88$  in S1, data not shown) with an onset of TWD, i.e. start of sustained stem shrinking, at  $\Psi_{\text{soil}}$  of around  $-0.2$  MPa (for P1 see Fig. 2a). However, the correlation between  $\Psi_{\text{soil}}$  and TWD was slightly less tight in study plots with unequally desiccating topsoil and deep soil layers (e.g. plot D2,  $R^2 = 0.77$ , data not shown).

### 3.4. Tree water status and transpiration

In plots P1–P3, both our proxies for transpiration,  $\delta^{13}\text{C}$  and  $\Psi_{\text{leaf\_md}} - \Psi_{\text{leaf\_pd}}$ , indicated a distinct reduction of transpiration with increasing drought stress along a  $\Psi_{\text{leaf\_pd}}$  gradient (Fig. 3).  $\delta^{13}\text{C}$  in water soluble leaf compounds was around  $-30\%$  at the moist end of the  $\Psi_{\text{leaf\_pd}}$  gradient ( $\Psi_{\text{leaf\_pd}} > -0.5$  MPa), then markedly increased to values of about  $-28\%$  at  $\Psi_{\text{leaf\_pd}}$  around  $-2.2$  MPa and stayed near  $-28\%$  towards the dry end of the studied gradient at  $-3.2$  MPa (Fig. 3a). This dynamics of  $\delta^{13}\text{C}$  suggests that transpiration strongly decreased between  $\Psi_{\text{leaf\_pd}} -0.5$  and  $-2.2$  MPa and remained on a low level below  $\Psi_{\text{leaf\_pd}}$  of  $-2.2$  MPa. However, the still present difference between  $\Psi_{\text{leaf\_md}}$  and  $\Psi_{\text{leaf\_pd}}$  below  $\Psi_{\text{leaf\_pd}}$  of  $-2.2$  MPa was a sign of not yet fully ceased leaf gas exchange (Fig. 3b). The daily fluctuations in  $\Psi_{\text{leaf}}$  fully disappeared at around  $-3.2$  MPa.

### 3.5. Drying of trees and soil

In plots P1–P3, decreases in  $\Psi_{\text{soil}}$  and  $\Psi_{\text{leaf\_pd}}$  were strongly related ( $R^2 = 0.86$ ), with  $\Psi_{\text{leaf\_pd}}$  always more negative than  $\Psi_{\text{soil}}$ , especially under severe drought (Fig. 4). In the most drought affected plot P2 (defoliation 40–75%), the mean  $\Psi_{\text{soil}}$  of the 49 soil samples from 18 sampling spots was  $-1.95$  MPa (data not shown). The small standard error of  $0.05$  MPa indicates that the soil was depleted strongly and homogeneously down to the parent rock (at ca.  $0.8$  m depth). In the slightly less drought affected plot P3 (defoliation 35–40%), the topsoil was similarly dry ( $-2.1$  MPa), but at a few sampling spots some plant available water was still left below  $1.0$  m depth, with a mean  $\Psi_{\text{soil}}$  of  $-0.85$  MPa at these moister locations.

### 3.6. Native embolism in 2018 and xylem vulnerability

Beech trees in plots P1–P3 had substantial native embolism at the peak of the 2018 drought (Fig. 5), increasing from about 30% PLC (at  $\Psi_{\text{leaf\_md}} -2.2$  MPa) to ca. 80% PLC (at  $\Psi_{\text{leaf\_md}} -3.2$  MPa). Unfortunately, no native embolism levels for moister conditions could be obtained, as sampling was conducted only during the 2018 drought period. Native embolism generally was more prevalent than predicted from the vulnerability curve, which indicated 50% PLC at water potentials around  $-3.4$  MPa (Fig. 5).

### 3.7. Crown dieback

In plots P1–P3, there was a moderate but significant positive linear relationship between the percentage of native embolism measured at the peak of the 2018 drought from branches in the lower crown and the percentage of crown dieback in 2019 (Fig. 6a). Moreover, the studied trees showed a strong positive linear relationship ( $R^2 = 0.69$ ) between the magnitude of early defoliation observed in the second half of September 2018 and crown dieback in 2019 (Fig. 6b).

Further, in June 2019, we observed several mature beech trees that had recently died scattered in the forest stand and about 30% mortality in the beech regeneration (tree height  $0.5$ – $3.0$  m) in the most drought affected plot P2 (data not shown). In plot P3 that was less affected by drought, no dead mature beech trees were observed but mortality of young beech trees was around 30%. No tree mortality was detected in plot P1 where drought was least intensive. In June 2020, none of the



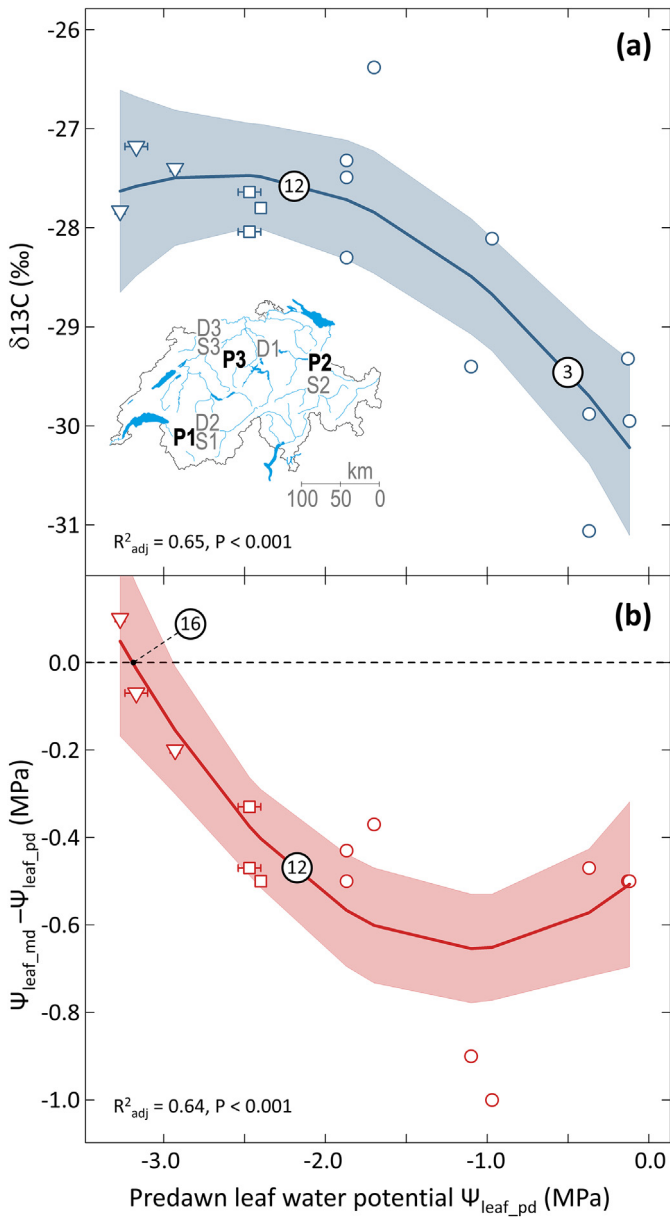


**Fig. 3.** Second-order polynomial relationships between predawn leaf water potential ( $\Psi_{leaf\_pd}$ ) and (a) predawn isotopic signature  $\delta^{13}C$  of water soluble leaf compounds and (b) the difference between leaf water potential at midday ( $\Psi_{leaf\_md}$ ) and predawn ( $\Psi_{leaf\_pd}$ ). Both relationships served as proxies for transpiration.  $\Psi_{leaf\_pd}$  represents the mean ( $\pm 1$  SE) of three leaves per tree from the studied beech trees (*F. sylvatica*) in plots P1 (circles, 2 trees, 5 sampling dates), P2 (triangles, 3 trees, 1 sampling date) and P3 (squares, 3 trees, 1 sampling date). Data were recorded on sunny days during 2017 and 2018. Note that for plot P1 only seven of totally ten data points are visible in (b) because of overlaying data points. The points ③, onset of reduced transpiration, ④, nearly zero transpiration and ⑥, cessation of leaf gas exchange, are used in the synthesis (Fig. 7).

affected study trees showed recovery from crown dieback, on the contrary, one study tree in the plot P2 had only one small living branch left in the lower crown.

**4. Discussion**

**4.1. Sequence of stress levels and thresholds during progressive drought**

In support of our first hypothesis, important responses of the investigated trees to progressive drought, such as reduced transpiration rate, early defoliation, native embolism and crown dieback were coherent across our study plots covering deep and shallow soils. This allowed

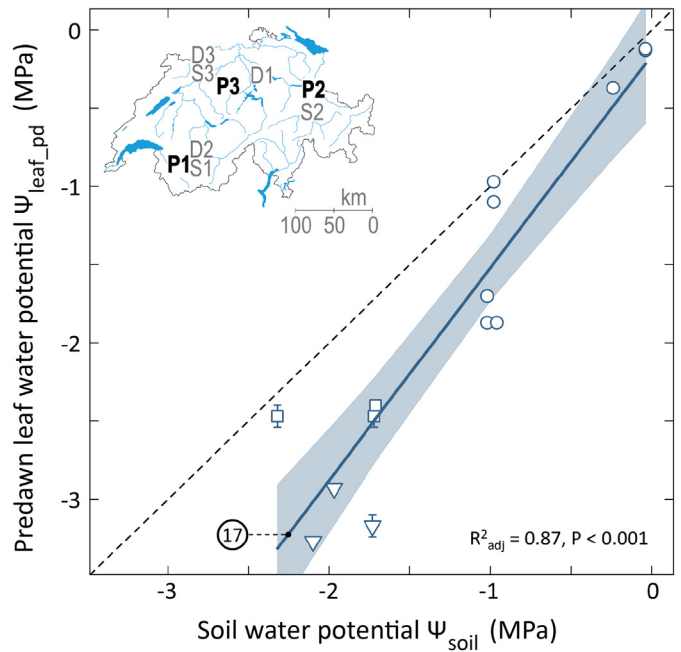


**Fig. 4.** Linear relationship between soil ( $\Psi_{soil}$ ) and predawn leaf water potential ( $\Psi_{leaf\_pd}$ ) of the studied beech trees (*F. sylvatica*) with increasing desiccation. Data were recorded in 2017 and 2018 in plot P1 (circles, 2 trees, 5 sampling dates) and at the peak of the 2018 drought in plots P2 (triangles, 3 trees, 1 sampling date) and P3 (squares, 3 trees, 1 sampling date).  $\Psi_{soil}$  is illustrated as the mean of all sampled soil depths down to 200 cm (P1) or down to parent rock (P2 and P3).  $\Psi_{leaf\_pd}$  represents the mean ( $\pm 1$  SE) of three leaves per tree. Note that for plot P1 only seven of totally ten data points are visible because of overlaying data points. The point ⑦, permanent wilting point, is used in the synthesis (Fig. 7).

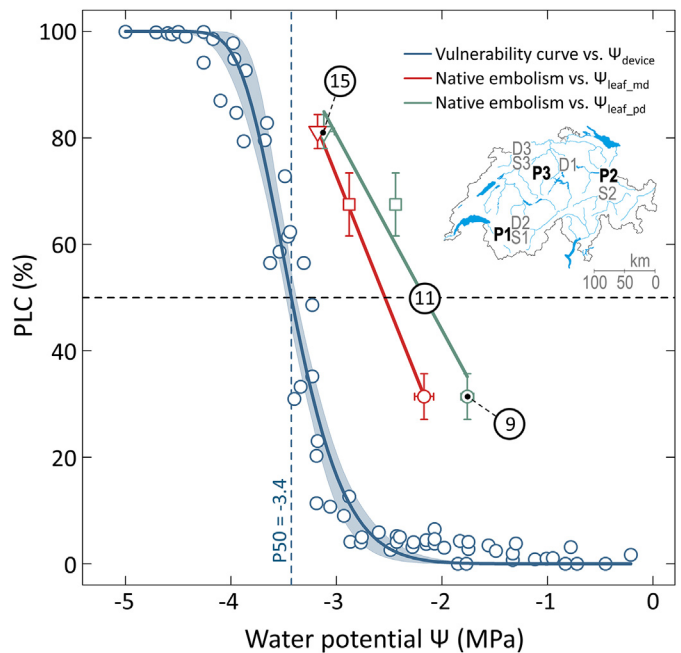


**Fig. 5.** Relationship between water potential ( $\Psi$ ) and percent loss of xylem conductance (PLC) in shoots of beech trees (*F. sylvatica*). Native embolism is shown for both  $\Psi_{leaf\_md}$  and  $\Psi_{leaf\_pd}$ , and each data point represents the mean ( $\pm 1$  SE) of values from one plot (P1 – circles, 5 trees; P2 – triangles, 3 trees ( $\Psi_{leaf}$ ), 5 trees (PLC); P3 – squares, 3 trees ( $\Psi_{leaf}$ ), 5 trees (PLC)). Xylem vulnerability is shown for branches of five trees from P1. Data were recorded at the peak of the 2018 drought. The points ⑨, ⑩ and ⑪, representing 30%, 50% and 80% native embolism, respectively, are used in the synthesis (Fig. 7).



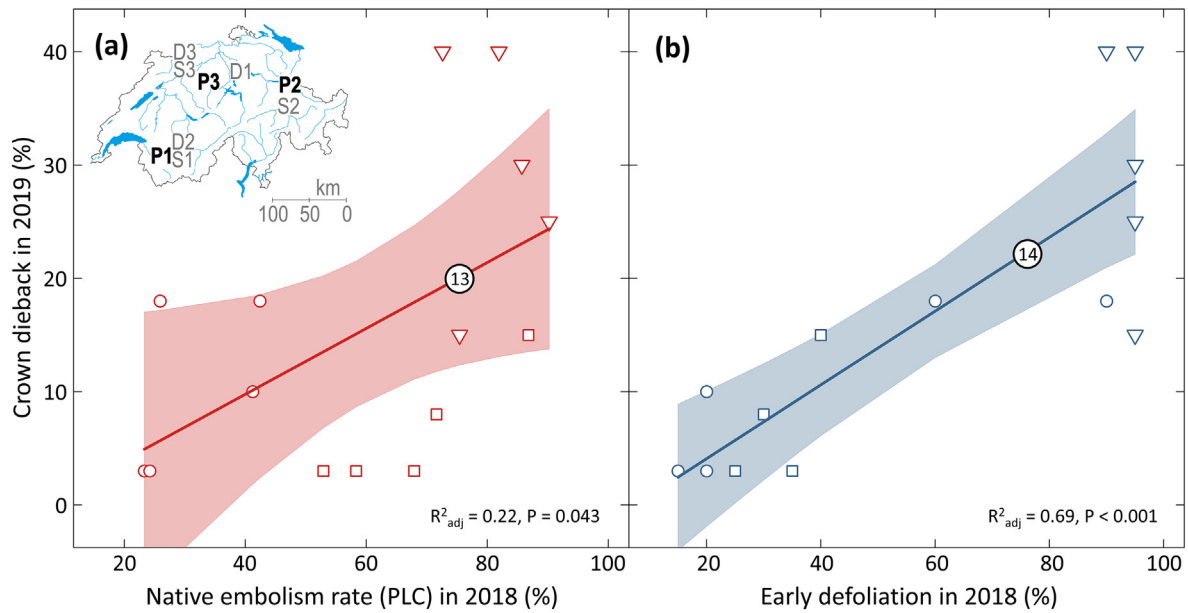


**Fig. 6.** Linear relationships between crown dieback in 2019, following the 2018 drought, and (a) native embolism in shoots at the drought peak in 2018 and (b) early defoliation in September 2018. Data are displayed for all 15 studied beech trees (*F. sylvatica*) in plots P1 (circles), P2 (triangles) and P3 (squares). Note that for plot P3 only four of totally five data points are visible in (b) because of overlaying data points. The points ⑬, 20% crown dieback and ⑭, 75% early defoliation, are used in the synthesis (Fig. 7).

us to summarise the drought responses of mature beech trees in a quantitative, empirically based scheme (Fig. 7) synthesising our results and additional data from literature. The observed physiological responses and stress symptoms suggested to distinguish five stress levels. In the following sections, we present the stress-level scheme and detail tree stress levels and related thresholds in response to decreasing  $\Psi_{\text{soil}}$  and  $\Psi_{\text{leaf\_pd}}$ .

#### 4.1.1. Level I: no signs of drought stress

At  $\Psi_{\text{leaf\_pd}} > -0.4$  MPa ( $\Psi_{\text{soil}} > -0.2$  MPa), no signs of drought stress were detectable in the study trees (Fig. 7). In this range, predawn TWD was zero (Fig. 2a) and our proxy for daily soil water uptake (delta  $\theta$ ) indicated a generally high water consumption of beech trees from all soil depths (Fig. 2b). The large variability in the amount of daily soil water uptake indicated a strong impact of atmospheric conditions driving transpiration and water uptake from moist soils. Following Larcher (2001), we consider full hydration of beech stems, i.e. a fully extended stem radius at predawn, optimal for tree performance where drought stress is negligible (Zweifel et al., 2005; Drew et al., 2011).

#### 4.1.2. Level II: moderate stress

At moderate drought stress ( $\Psi_{\text{leaf\_pd}}$  of  $-0.4$  to  $-1.3$  MPa;  $\Psi_{\text{soil}}$  of  $-0.2$  to  $-0.8$  MPa), our data indicate that beech trees restricted water losses by stomatal regulation. The values of daily soil water uptake were clearly reduced at all soil depths compared to the no-stress level (Fig. 2b), corresponding to decreasing transpiration (Fig. 3a). Stem shrinkage indicated increasing tree water deficits (Fig. 2a). We defined the stress threshold *T-II* to be at around  $\Psi_{\text{leaf\_pd}} -0.4$  MPa, and thus at the onset of markedly reduced water uptake from all soil depths (Figs. 2b,7;①) where stems started to shrink (Figs. 2a,7;②).

The onset of a persistent stem shrinkage over more than 24 h represents an important point in terms of plant performance along a drought stress gradient because no stem growth is possible during stem shrinkage (Zweifel et al., 2016), owing to insufficient turgor for cell enlargement (Taiz and Zeiger, 2010; Körner, 2015). An onset of water saving, i.e. of reduced transpiration, around  $\Psi_{\text{leaf\_pd}}$  of  $-0.5$  MPa (Figs. 3a,7;③) was likewise found by Pflug et al. (2018) for juvenile beech trees and according to Aranda et al. (2005) leaf conductance was reduced by as much as 45% at  $\Psi_{\text{leaf\_pd}}$  of about  $-0.8$  MPa (Fig. 7;④). Drought induced reductions of soil water uptake and

transpiration were often attributed to a relatively high vulnerability of root xylem to cavitation, i.e. to large losses of root conductivity (e.g. Jackson et al., 2000; Sperry, 2000; Sperry et al., 2002; Domec et al., 2010). However, a recent study shows that different parts of young beech trees have similar vulnerabilities to cavitation and that beech roots have a relatively low P50 value of around  $-2.75$  MPa (Losso et al., 2019). Moreover, novel findings indicate that soil water uptake by roots could be reduced by a low hydraulic conductivity in the rhizosphere, even in relatively moist soils (Carminati et al., 2020).

#### 4.1.3. Level III: high stress

Under high drought stress ( $\Psi_{\text{leaf\_pd}}$  of  $-1.3$  to  $-2.1$  MPa;  $\Psi_{\text{soil}}$  of  $-0.8$  to  $-1.4$  MPa), beech trees avoided water loss through a distinct reduction of transpiration (Fig. 3a) and by defoliation (Fig. 1a). Soil water uptake was very low (Fig. 2b), which was also reflected in a low stomatal conductance of around 10–20% of maximal values (Fig. 7;⑤,⑩) found by Leuzinger et al. (2005) and Peiffer et al. (2014). Despite stomata were nearly closed, native embolism set in (Fig. 5). We set the stress threshold *T-III* at  $\Psi_{\text{leaf\_pd}}$  of  $-1.3$  MPa (Fig. 7), where soil water uptake (Figs. 2b,7;⑤) decreased to very low values and where native embolism (Fig. 7,⑥) and early defoliation (Figs. 1,7;⑦) started.

While stomatal control started already at a relatively high  $\Psi_{\text{leaf\_pd}}$  of about  $-0.5$  MPa (Figs. 3a,7;③), a strong reduction in stomatal conductance was not reached until  $\Psi_{\text{leaf\_pd}}$  was as low as  $-1.4$  MPa (Fig. 7,⑧), and thus near the onset of native embolism (Fig. 7,⑥). The onset of xylem embolism close to or even within the operating range of stomatal regulation can be interpreted as a characteristic of trees with a small safety margin against drought (Martin-StPaul et al., 2017).

#### 4.1.4. Level IV: very high stress

Very high drought stress ( $\Psi_{\text{leaf\_pd}}$  of  $-2.1$  to  $-2.8$  MPa;  $\Psi_{\text{soil}}$  of  $-1.4$  to  $-1.9$  MPa) was assumed beyond the stress threshold *T-IV*, where native embolism exceeded 50% (Figs. 5,7;⑩). At this stress level, stomata were most likely nearly fully closed (Figs. 3,7;⑩). This level of stress induced physiological damages leading to early defoliation and also resulted in crown dieback in the following year (Figs. 6,7).

In the context of water saving, drought-induced defoliation was observed to be advantageous in the short term, and crown dieback in the long term for some tree species (Tyree et al., 1993; Rood et al., 2000).

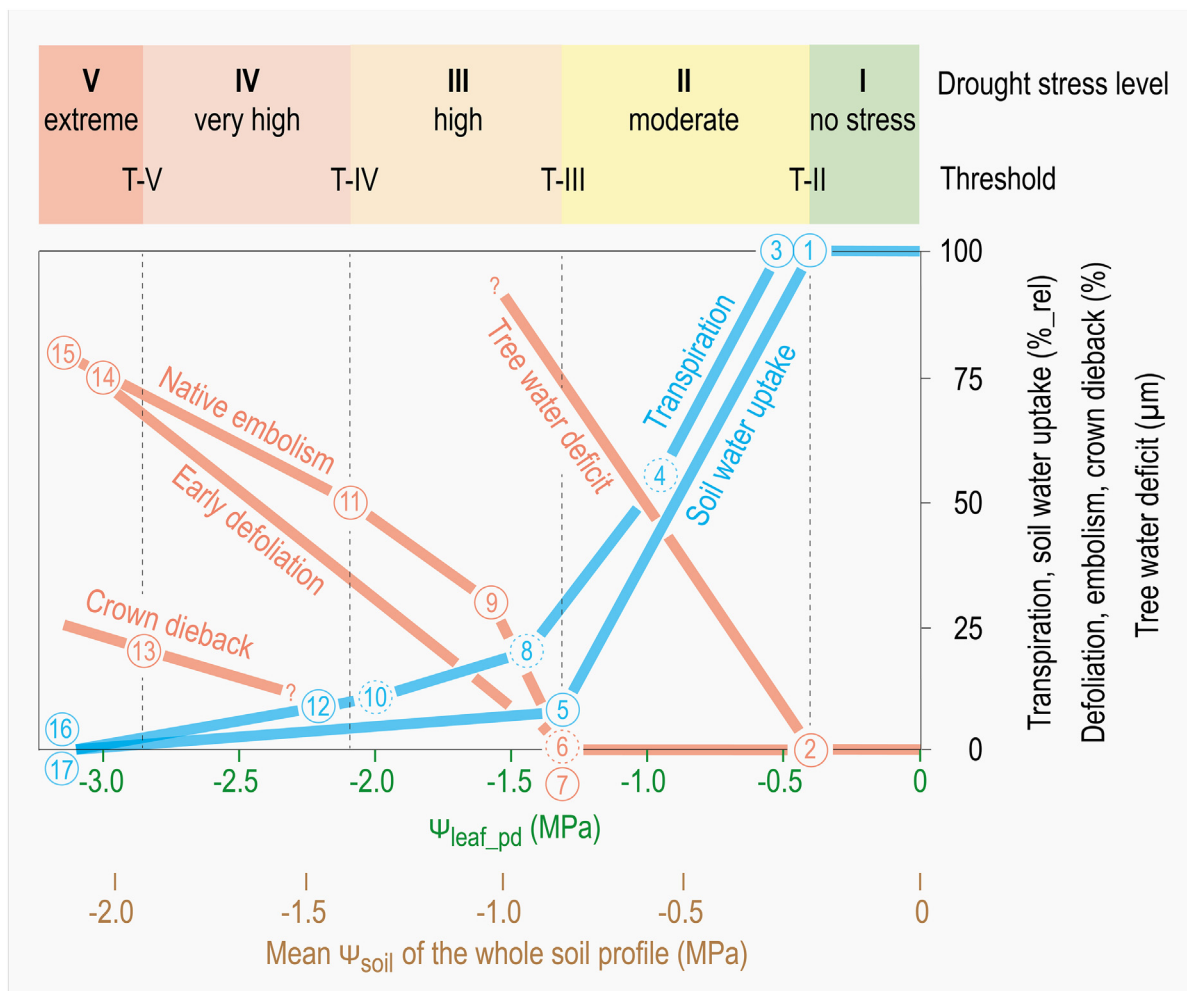


**Fig. 7.** Schematic synthesis of physiological responses of mature beech trees (*F. sylvatica*) to progressive drought. The derivation of the five stress levels and the positioning of the thresholds are based on important physiological responses and stress symptoms (①–⑰) which are numbered according to their occurrence under decreasing water potential ( $\Psi$ ). Note that the stress levels and thresholds are expressed relative to soil ( $\Psi_{\text{soil}}$ ) and predawn leaf water potential ( $\Psi_{\text{leaf\_pd}}$ ) owing to the high correlation between  $\Psi_{\text{soil}}$  and  $\Psi_{\text{leaf\_pd}}$  (Fig. 4). Values for  $\Psi_{\text{leaf\_md}}$  can be derived from Fig. 3b. Data source of ①–⑰: ① Onset of reduced soil water uptake (Fig. 2b), ② Onset of stem shrinkage and cessation of growth (Fig. 2a), ③ Onset of reduced transpiration (Fig. 3a), ④ 45% reduction of leaf conductance (Aranda et al. (2005)), ⑤ 97% reduction of soil water uptake (Fig. 2b), ⑥ Onset of xylem embolism (Hacke and Sauter (1995) and Fig. 3b), ⑦ Onset of early defoliation (Fig. 1a), ⑧ 80% reduction of maximal stomatal conductance (Leuzinger et al. (2005)), ⑨ 30% native embolism (Fig. 5), ⑩ 90% reduction of maximal stomatal conductance (Peiffer et al. (2014)), ⑪ 50% native embolism (Fig. 5), ⑫ Nearly zero transpiration (Fig. 3), ⑬ Crown dieback ca. 20% (Figs. 5.6a), ⑭ 75% early defoliation (Figs. 5.6a,b), ⑮ 80% native embolism (Fig. 5), ⑯ Cessation of leaf gas exchange (Fig. 3b) indicating the permanent wilting point ⑰ (Fig. 4). The points ④, ⑥, ⑧ and ⑩ from the literature refer only to the  $\Psi_{\text{leaf\_pd}}$  axis as  $\Psi_{\text{soil}}$  is not known.

In our study, native embolism and early defoliation started at a similar  $\Psi_{\text{leaf}}$  (Fig. 7; ⑥, ⑦) and increased simultaneously, suggesting that defoliation started too late to protect the xylem from high cavitation rates. These results are consistent with findings regarding several tropical species (Wolfe et al., 2016). Therefore, drought-induced defoliation in beech trees may be interpreted to be a consequence of hydraulic failure, i.e. dehydration, rather than a strategy to prevent hydraulic failure.

#### 4.1.5. Level V: extreme stress

The threshold to extreme stress was defined to be at around  $\Psi_{\text{leaf\_pd}}$  of  $-2.8$  MPa ( $\Psi_{\text{soil}}$  of  $-1.9$  MPa), where mean crown dieback in the year after the drought exceeded 20% (Figs. 6a,7; ⑬). At this stress level, native embolism increased to values  $>80\%$  (Figs. 5,7; ⑮) and transpiration ceased (Figs. 3b,7; ⑰). Therefore, beech trees were considered to be close to their limit to maintain physiological functioning and at risk to die from water shortage.

Small differences between daily  $\Psi_{\text{leaf\_pd}}$  and  $\Psi_{\text{leaf\_md}}$  indicated ongoing loss of water through the leaf's surface (stomatal or cuticular transpiration) above  $\Psi_{\text{leaf\_pd}}$  of  $-3.2$  MPa (Fig. 3b). However, at around this value, the daily fluctuations in  $\Psi_{\text{leaf}}$  ceased (Fig. 3b; ⑰), which suggests

according to the theoretical frameworks of Hinckley et al. (1978) and Martinez-Vilalta et al. (2014) the cessation of leaf gas exchange. Our interpretation of this value as the PWP (Figs. 4,7; ⑰) is supported by the uniformly low  $\Psi_{\text{soil}}$  in the whole rooting zone (plot P2), indicating that no water uptake was possible anymore. Thus, while beech trees started to show early defoliation at  $\Psi_{\text{soil}}$  of around  $-0.8$  MPa (Figs. 1,7; ⑦), the PWP at  $\Psi_{\text{soil}}$  of about  $-2.2$  MPa (Figs. 4,7; ⑰) represented the end point of transpiration-induced soil water extraction by beech roots. The disruption of the capillary continuum between the soil and the roots may be responsible for the increasingly limited water uptake from drying soils (Meinzer et al., 2013; Johnson et al., 2018; Poyatos et al., 2018; Körner, 2019; Rodriguez-Dominguez and Brodrigg, 2020) and also for the observed increase in the divergence of  $\Psi_{\text{leaf\_pd}}$  and  $\Psi_{\text{soil}}$  towards the PWP (Fig. 4). This indicates that trees rely more and more on internally stored water when drought progresses (Körner, 2019) because of hydraulic decoupling of plant and soil, i.e. biosphere and pedosphere.

With our multi-spheric approach that used data from the atmo-, bio-, hydro-, and lithosphere over the whole range of water availability in beech forests, we were able to establish an empirical scheme that reveals the stress behaviour of mature beech trees under natural drought

conditions. Stress intensity as measured by the degree of physiological downregulation in beech trees was clearly related to plant available water in the investigated spheres indicating hydraulic interconnection of these spheres. Therefore, we were able to refer plant stress intensity to the water potential in both, plant and soil (Fig. 7), even though a certain hydraulic decoupling of plant and soil was observed towards drier conditions. In support of our second hypothesis, important physiological responses and stress symptoms enabled us to assign the stress behaviour to distinct stress levels that are related to tree performance. Overall, the physiological drought responses that form the basis of our scheme fit well with values reported in the literature for mature beech trees, supporting the general validity of the scheme. Above  $-1.6$  MPa, our stress-level scheme is in line with, for example, the relationship between  $\Psi_{\text{leaf\_pd}}$  and TWD found by Dietrich et al. (2018), the course of  $\Psi_{\text{leaf\_md}}$  and  $\Psi_{\text{leaf\_pd}}$  (Leuzinger et al., 2005; Dietrich et al., 2019) and the range of  $\delta^{13}\text{C}$  values (Bögelein et al., 2012). High consistency was likewise found for xylem vulnerability (Schuldt et al., 2016; Stojnic et al., 2018) and for defoliation and crown-dieback, that were never observed at  $\Psi_{\text{leaf\_pd}}$  above  $-1.6$  MPa. Moreover, there was a good agreement between soil water uptake from our study and leaf gas exchange (transpiration) from the literature (Fig. 7). While mature beech trees always seem to follow similar physiological trajectories under mild to moderate drought conditions, future research will show how robust our scheme is under severe drought, i.e. at  $\Psi_{\text{leaf\_pd}}$  below  $-1.6$  MPa. In this very dry range, our findings are in line with a novel published first overview of the 2018 drought effects on Central European forests where drought affected mature beech trees had similarly low  $\Psi_{\text{leaf}}$  as in our study (Schuldt et al., 2020).

#### 4.2. Stress frequency and stress duration

Our stress-level scheme (Fig. 7) is based on stress intensity and implicitly also involves a timeline of drought. In this section, we try to show more explicitly how stress frequency and stress duration may relate to the defined stress levels. The stress level 2, where water losses are controlled by dynamic stomatal regulation without harming the tree hydraulic system, is considered to occur frequently in mature beech trees. At the plot P1, for example, this stress level was largely crossed once or even several times in each vegetation period between 2014 and 2017 (Fig. 2b). The stress levels 3–5, in contrast, seem to occur less frequently. We found only one reference that reported  $\Psi_{\text{leaf\_pd}}$  below  $-1.6$  MPa and related drought stress symptoms for mature beech trees (Peiffer et al., 2014). To this date, such high levels of stress probably occurred mainly at the dry distribution edge of European beech while beech sites with a better water supply were affected only during severe drought events. In 2018, it took 3–4 months of severe atmospheric drought until the shallow soils of the plots S1–S3 had reached stress level 3, i.e. the threshold of early defoliation (Fig. 1a). In the plots P2 and P3, the duration between the onset of early defoliation (start of level 3 around mid of July) and the formation of 65–80% native embolism (levels 4–5) was about one month. In the plot P2, beech crowns were affected by up to 40% dieback in June 2019 even though the topsoil was relatively moist from 21. August 2018 onwards and therefore some shrub species sprouted again owing to this stress release. Apparently, the heavily embolised beech trees in this plot were not able to recover during these more favourable autumnal conditions. We therefore conclude that during the severe drought 2018, an exposure to the stress levels 3–5 of about one month was sufficiently long to cause high levels of native embolism and subsequent crown dieback in mature beech trees.

#### 4.3. Native embolism indicates higher drought stress than predicted from the xylem vulnerability curve

Interestingly, native embolism was overall more prevalent at a given  $\Psi$  than predicted from the vulnerability curve (Fig. 5). This discrepancy

was not an artefact from cavitation fatigue (Hacke et al., 2001) because the branches used for both measurements were exposed to the same influences before sampling. Furthermore, the similarity of vulnerability thresholds in different studies (e.g. Schuldt et al., 2016; Stojnic et al., 2018) and their consistency with our study that used branches which previously suffered native embolism indicates a lack of relevant cavitation fatigue in European beech. We rather see the following four reasons for the observed discrepancy between native embolism and vulnerability curve: First,  $\Psi_{\text{leaf}}$  was measured in the lower crown, while lower  $\Psi$  values might have been reached in more exposed crown parts. However, data collection in the upper crown was not possible, owing to excessive defoliation. Second, although  $\Psi_{\text{leaf}}$  was assessed at the peak of drought on hot and sunny days, measurements may not represent the minimum  $\Psi$  reached during the drought period. Third, the long-lasting exposure to relatively low  $\Psi_{\text{leaf}}$  under natural conditions may impact xylem embolism differently than the short exposure in the laboratory (i.e. cavitron). Fourth, a portion of the measured native embolism may originate from previous stress events that left embolisms in older tree rings. In our stress-level scheme, we referred to measured native embolism, as the 2018 drought offered the rare opportunity to include a parameter relevant *in planta*. We thus suggest that vulnerability curves, although important e.g. for species comparisons, might not sufficiently reflect stress conditions in forests under drought.

#### 4.4. Beech is vulnerable to drought

The observed drought stress behaviour of beech trees indicates that European beech is vulnerable to drought. Even if it starts to save water at an early stage of drought (at  $\Psi_{\text{leaf\_pd}}$  of around  $-0.5$  MPa), transpirational water loss is still ongoing at substantial levels of drought-induced defoliation and native embolism. Our findings further suggest that early defoliation may result in, and can even be used as a predictor for, crown dieback in the following year. Crown dieback impacts the vitality of beech trees and probably makes them more susceptible to pathogens and harmful insects (Jung, 2009) and ultimately whole-tree mortality (Chakraborty et al., 2017).

#### 4.5. Implications for the future beech distribution

Temperature and natural disturbances such as drought are predicted to increase globally in the future (McDowell et al., 2020). Therefore, drought vulnerable tree species such as European beech are expected to suffer from critical stress levels and subsequent damages more frequently at many forest sites. More generally, natural disturbances and biotic attacks are hypothesized to induce shifts in forest dynamics by changing mortality, growth and recruitment of tree species, leading to species shifts and shorter-statured forests in the long-term (McDowell et al., 2020), with predominantly negative effects on forest ecosystem services. Shifting forest dynamics may reduce, for example, the economic value of forest land (Hanewinkel et al., 2013), carbon sequestration (McDowell et al., 2020), and the protection capacity against natural hazards. Forest management to assure important forest ecosystem services in the long-term is challenging under perpetual shifts in forest dynamics. One major source of current uncertainties in forest planning can be ascribed to deficient knowledge of the drought vulnerability of individual tree species and related migrations of species ecological niches. An implementation of our stress-level scheme in vegetation models could contribute to a more consistent projection of how future drought could affect the distribution of European beech, as it reflects changes in tree performance and competitiveness with decreasing  $\Psi$ . Anticipating changes in the future distribution of European beech and other tree species can help to reduce uncertainties in forest management and planning.

Reliable predictions of species distributions, however, require not only a sound knowledge of species stress behaviour but also accurate environmental data. Soil water reserves turned out to be important to mitigate atmospheric drought effects at the study plots during the severe



meteorological drought in 2018. In support of our third hypothesis, beech trees on deep soils with a high AWC took advantage of the water reserves in deep soil layers (until 2 m depth, at least) and showed no or only weak stress symptoms. On shallow soils, in contrast, the stress symptoms were more pronounced because of water shortage resulting from severe soil drying. With an AWC that amounted to only 15–60% of the precipitation sum between April and September 2018, the water reserves of the shallow soils were too small to effectively mitigate atmospheric drought effects. These findings suggest to use AWC in drought stress studies and in vegetation models because of its potential to modify atmospheric drought effects on plants. For a reliable estimate of AWC, several soil properties over possibly the whole depth of the rooting zone are needed. If soil depth or important soil properties are neglected in AWC estimates (e.g. D'Orangeville et al., 2018), one cannot expect meaningful relations between these surrogate AWCs and drought reactions of forests. Soil water is expected to influence species distributions especially in forest biomes where it can strongly modify atmospheric drought effects, and thus where AWC has a high spatial variation and where it is depleted and replenished periodically. Such conditions prevail, for example, in many forested areas of Western Europe, where Piedallu et al. (2011) showed that AWC considerably improved predictions of forest productivity. Moreover, soil water reserves helped to better explain seasonal vegetation dynamics such as canopy greenness (Piedallu et al., 2019). This is in line with our findings, that soil water reserves mitigate drought stress in mature beech trees by compensating sporadic atmospheric water shortage. In view of a further intensification of summer drought periods, soil water reserves will become increasingly important in dampening plant drought stress at many forest sites.

## 5. Conclusions

We investigated poorly understood hydraulics of mature European beech trees with a relevant tree physiological and environmental data set from natural beech forests on a wide variety of soils, including drought intensities that triggered stress symptoms and tree damage. We combined data from the atmo-, bio-, hydro-, and lithosphere and developed an empirical scheme to quantify drought stress in mature beech trees up to the permanent wilting point. The stress levels consider multiple physiological responses, both above and below ground, and are linked to tree performance, e.g. growth, leaf wilting or crown dieback. Our stress-level scheme complements the knowledge of critical thresholds during drought stress in tree species. It could contribute to more realistic predictions of the beech distribution under future climate and to reduce current uncertainties in forest management and planning. Moreover, our study highlights the importance of water reserves in deep soil layers in mitigating atmospheric drought effects on beech trees. Consequently, the quality of predicted future beech distributions could be improved by including reliable data on local soil water holding capacity and soil water availability. More generally, our approach could serve as a model for future investigations of the drought stress behaviour in other tree species.

## CRedit authorship contribution statement

**Lorenz Walthert:** Conceptualization, Methodology, Investigation, Writing. **Andrea Ganthaler:** Investigation, Writing. **Stefan Mayr:** Resources, Writing. **Matthias Saurer:** Investigation, Resources, Writing. **Peter Waldner:** Investigation, Writing. **Marco Walsler:** Investigation. **Roman Zweifel:** Investigation, Resources, Writing. **Georg von Arx:** Conceptualization, Methodology, Formal analysis, Writing.

## Declaration of competing interest

The authors declare that they have no known competing financial interests or personal relationships that could have appeared to influence the work reported in this paper.

## Acknowledgements

We thank Roger Köchli for field work, Luzi Bernhard for calculating the meteorological anomalies of 2018, Melissa Dawes for language editing help and the Swiss Federal Office for the Environment (FOEN) for partly funding logging infrastructure and maintenance costs for TreeNet (Grants 00.0365.PZIO427-0562 and 09.0064.PJ/R301-0223).

## Data accessibility

The data of this publication are available on: <https://www.doi.org/10.16904/envidat.167>

## References

- Adams, H.D., Zeppel, M.J.B., Anderegg, W.R.L., Hartmann, H., Landhauer, S.M., Tissue, D.T., Huxman, T.E., Hudson, P.J., Franz, T.E., Allen, C.D., et al., 2017. A multi-species synthesis of physiological mechanisms in drought-induced tree mortality. *Nature Ecology & Evolution* 1, 1285–1291.
- Allen, C.D., Macalady, A.K., Chenchouni, H., Bachelet, D., McDowell, N., Venetier, M., Kitzberger, T., Rigling, A., Breshears, D.D., Hogg, E.H., et al., 2010. A global overview of drought and heat-induced tree mortality reveals emerging climate change risks for forests. *For. Ecol. Manag.* 259, 660–684.
- Aranda, I., Gil, L., Pardos, J.A., 2005. Seasonal changes in apparent hydraulic conductance and their implications for water use of European beech (*Fagus sylvatica* L.) and sessile oak (*Quercus petraea* (Matt.) Liebl.) in South Europe. *Plant Ecol.* 179, 155–167.
- Aussenac, G., Granier, A., 1978. Quelques résultats de cinétique journalière du potentiel de sève chez les arbres forestiers. *Ann. For. Sci.* 35, 19–32.
- Backes, K., Leuschner, C., 2000. Leaf water relations of competitive *Fagus sylvatica* and *Quercus petraea* trees during 4 years differing in soil drought. *Canadian Journal of Forest Research-Revue Canadienne De Recherche Forestiere* 30, 335–346.
- Barigah, T.S., Charrier, O., Douris, M., Bonhomme, M., Herbette, S., Ameglio, T., Fichot, R., Brignolas, F., Cochar, H., 2013. Water stress-induced xylem hydraulic failure is a causal factor of tree mortality in beech and poplar. *Ann. Bot.* 112, 1431–1437.
- Bartlett, M.K., Klein, T., Jansen, S., Choat, B., Sack, L., 2016. The correlations and sequence of plant stomatal, hydraulic, and wilting responses to drought. *Proc. Natl. Acad. Sci. U. S. A.* 113, 13098–13103.
- Beikircher, B., Mayr, S., 2016. Avoidance of harvesting and sampling artefacts in hydraulic analyses: a protocol tested on *Malus domestica*. *Tree Physiol.* 36, 797–803.
- Beikircher, B., Ameglio, T., Cochar, H., Mayr, S., 2010. Limitation of the Cavitrone technique by conifer pit aspiration. *J. Exp. Bot.* 61, 3385–3393.
- Bögelein, R., Hassdenteufel, M., Thomas, F.M., Werner, W., 2012. Comparison of leaf gas exchange and stable isotope signature of water-soluble compounds along canopy gradients of co-occurring Douglas-fir and European beech. *Plant Cell and Environment* 35, 1245–1257.
- Bréda, N., Granier, A., Barataud, F., Moyne, C., 1995. Soil-water dynamics in an oak stand. 1. Soil-moisture, water potentials and water-uptake by roots. *Plant Soil* 172, 17–27.
- Bréda, N., Huc, R., Granier, A., Dreyer, E., 2006. Temperate forest trees and stands under severe drought: a review of ecophysiological responses, adaptation processes and long-term consequences. *Ann. For. Sci.* 63, 625–644.
- Brunner, M.I., Liechti, K., Zappa, M., 2019. Extremeness of recent drought events in Switzerland: dependence on variable and return period choice. *Nat. Hazards Earth Syst. Sci.* 19, 2311–2323.
- Bunce, J.A., Miller, L.N., Chabot, B.F., 1977. Competitive exploitation of soil-water by 5 eastern North-American tree species. *Bot. Gaz.* 138, 168–173.
- Carminati, A., Ahmed, M.A., Zarebanadkouki, M., Cai, G.H., Lovric, G., Javaux, M., 2020. Stomatal closure prevents the drop in soil water potential around roots. *New Phytol.* 226, 1541–1543.
- Carrière, S.D., Martin-StPaul, N.K., Cakpo, C.B., Patris, N., Gillon, M., Chalikakis, K., Doussan, C., Olioso, A., Babic, M., Jouineau, A., et al., 2020. The role of deep vadose zone water in tree transpiration during drought periods in karst settings - insights from isotopic tracing and leaf water potential. *Sci. Total Environ.* 699.
- Cavin, L., Mountford, E.P., Peterken, G.F., Jump, A.S., 2013. Extreme drought alters competitive dominance within and between tree species in a mixed forest stand. *Funct. Ecol.* 27, 1424–1435.
- Chakraborty, T., Saha, S., Matzarakis, A., Reif, A., 2017. Influence of multiple biotic and abiotic factors on the crown die-back of European beech trees at their drought limit. *Flora* 229, 58–70.
- Choat, B., Jansen, S., Brodribb, T.J., Cochar, H., Delzon, S., Bhaskar, R., Bucci, S.J., Feild, T.S., Gleason, S.M., Hacke, U.G., et al., 2012. Global convergence in the vulnerability of forests to drought. *Nature* 491, 752–755.
- Choat, B., Brodribb, T.J., Brodersen, C.R., Duursma, R.A., Lopez, R., Medlyn, B.E., 2018. Triggers of tree mortality under drought. *Nature* 558, 531–539.
- Cochar, H., Damour, G., Bodet, C., Tharwat, I., Poirier, M., Ameglio, T., 2005. Evaluation of a new centrifuge technique for rapid generation of xylem vulnerability curves. *Physiol. Plant.* 124, 410–418.
- Dai, A.G., 2013. Increasing drought under global warming in observations and models. *Nat. Clim. Chang.* 3, 52–58.
- Delzon, S., Cochar, H., 2014. Recent advances in tree hydraulics highlight the ecological significance of the hydraulic safety margin. *New Phytol.* 203, 355–358.
- Dietrich, L., Zweifel, R., Kahmen, A., 2018. Daily stem diameter variations can predict the canopy water status of mature temperate trees. *Tree Physiol.* 38, 941–952.



- Dietrich, L., Delzon, S., Hoch, G., Kahmen, A., 2019. No role for xylem embolism or carbohydrate shortage in temperate trees during the severe 2015 drought. *J. Ecol.* 107, 334–349.
- Domec, J.C., Schafer, K., Oren, R., Kim, H.S., McCarthy, H.R., 2010. Variable conductivity and embolism in roots and branches of four contrasting tree species and their impacts on whole-plant hydraulic performance under future atmospheric CO<sub>2</sub> concentration. *Tree Physiol.* 30, 1001–1015.
- D'Orangeville, L., Maxwell, J., Kneeshaw, D., Pederson, N., Duchesne, L., Logan, T., Houle, D., Arseneault, D., Beier, C.M., Bishop, D.A., et al., 2018. Drought timing and local climate determine the sensitivity of eastern temperate forests to drought. *Glob. Chang. Biol.* 24, 2339–2351.
- Drew, D.M., Richards, A.E., Downes, G.M., Cook, G.D., Baker, P., 2011. The development of seasonal tree water deficit in *Callitris intratropica*. *Tree Physiol.* 31, 953–964.
- Duurmsma, R., Choat, B., 2017. Fitplc - an R package to fit hydraulic vulnerability curves. *Journal of Plant Hydraulics* 4, e002.
- Farquhar, G.D., Ehleringer, J.R., Hubick, K.T., 1989. Carbon isotope discrimination and photosynthesis. *Annu. Rev. Plant Physiol. Plant Mol. Biol.* 40, 503–537.
- Fotelli, M.N., Nahm, M., Radoglou, K., Rennenberg, H., Halyvopoulos, G., Matzarakis, A., 2009. Seasonal and interannual ecophysiological responses of beech (*Fagus sylvatica*) at its south-eastern distribution limit in Europe. *For. Ecol. Manag.* 257, 1157–1164.
- Fulton, A., Buchner, R., Olson, B., Schwankl, L., Gilles, C., Bertagna, N., Walton, J., Shackel, K., 2001. Rapid equilibration of leaf and stem water potential under field conditions in almonds, walnuts, and prunes. *Horttechnology* 11, 609–615.
- van Genuchten, M.T., Leij, F.J., Yates, S.R., 1991. The RETC Code for Quantifying the Hydraulic Functions of Unsaturated Soils. U. S. Environmental Protection Agency EPA, Ada, OK, USA.
- Gobiet, A., Kotlarski, S., Beniston, M., Heinrich, G., Rajczak, J., Stoffel, M., 2014. 21st century climate change in the European Alps - a review. *Sci. Total Environ.* 493, 1138–1151.
- Hacke, U., Sauter, J.J., 1995. Vulnerability of xylem to embolism in relation to leaf water potential and stomatal conductance in *Fagus sylvatica* f. *purpurea* and *Populus balsamifera*. *J. Exp. Bot.* 46, 1177–1183.
- Hacke, U.G., Stiller, V., Sperry, J.S., Pittermann, J., McCulloh, K.A., 2001. Cavitation fatigue. Embolism and refilling cycles can weaken the cavitation resistance of xylem. *Plant Physiol.* 125, 779–786.
- Hanewinkel, M., Cullmann, D.A., Schelhaas, M.J., Nabuurs, G.J., Zimmermann, N.E., 2013. Climate change may cause severe loss in the economic value of European forest land. *Nat. Clim. Chang.* 3, 203–207.
- Hartmann, H., Moura, C.F., Anderegg, W.R.L., Ruehr, N.K., Salmon, Y., Allen, C.D., Arndt, S.K., Breshears, D.D., Davi, H., Galbraith, D., et al., 2018. Research frontiers for improving our understanding of drought-induced tree and forest mortality. *New Phytol.* 218, 15–28.
- Hinckley, T.M., Lassoie, J.P., Running, S.W., 1978. Temporal and spatial variations in water status of forest trees. *For. Sci.* 24, 1–72.
- Jackson, R.B., Sperry, J.S., Dawson, T.E., 2000. Root water uptake and transport: using physiological processes in global predictions. *Trends Plant Sci.* 5, 482–488.
- Johnson, D.M., Domec, J.C., Berry, Z.C., Schwantes, A.M., McCulloh, K.A., Woodruff, D.R., Polley, H.W., Wortemann, R., Swenson, J.J., Mackay, D.S., et al., 2018. Co-occurring woody species have diverse hydraulic strategies and mortality rates during an extreme drought. *Plant Cell and Environment* 41, 576–588.
- Jung, T., 2009. Beech decline in Central Europe driven by the interaction between *Phytophthora* infections and climatic extremes. *For. Pathol.* 39, 73–94.
- Köcher, P., Gebauer, T., Horna, V., Leuschner, C., 2009. Leaf water status and stem xylem flux in relation to soil drought in five temperate broad-leaved tree species with contrasting water use strategies. *Ann. For. Sci.* 66, 101.
- Kolb, T.E., Matyssek, R., 2001. Limitations and perspectives about scaling ozone impacts in trees. *Environ. Pollut.* 115, 373–392.
- Körner, C., 2015. Paradigm shift in plant growth control. *Curr. Opin. Plant Biol.* 25, 107–114.
- Körner, C., 2019. No need for pipes when the well is dry—a comment on hydraulic failure in trees. *Tree Physiol.* 39, 695–700.
- Larcher, W., 2001. *Ökophysiologie der Pflanzen*. Ulmer Verlag, Stuttgart, DE.
- Lehmann, M.M., Gamarra, B., Kahmen, A., Siegwolf, R.T.W., Saurer, M., 2017. Oxygen isotope fractionations across individual leaf carbohydrates in grass and tree species. *Plant Cell and Environment* 40, 1658–1670.
- Lemoine, D., Cochard, H., Granier, A., 2002. Within crown variation in hydraulic architecture in beech (*Fagus sylvatica* L.): evidence for a stomatal control of xylem embolism. *Ann. For. Sci.* 59, 19–27.
- Leuzinger, S., Zotz, G., Ashhoff, R., Körner, C., 2005. Responses of deciduous forest trees to severe drought in Central Europe. *Tree Physiol.* 25, 641–650.
- Losso, A., Nardini, A., Damon, B., Mayr, S., 2018. Xylem sap chemistry: seasonal changes in timberline conifers *Pinus cembra*, *Picea abies*, and *Larix decidua*. *Biol. Plant.* 62, 157–165.
- Losso, A., Bar, A., Damon, B., Dullin, C., Ganthaler, A., Petruzzellis, F., Savi, T., Tromba, G., Nardini, A., Mayr, S., et al., 2019. Insights from in vivo micro-CT analysis: testing the hydraulic vulnerability segmentation in *Acer pseudoplatanus* and *Fagus sylvatica* seedlings. *New Phytol.* 221, 1831–1842.
- Martinez-Vilalta, J., Lloret, F., 2016. Drought-induced vegetation shifts in terrestrial ecosystems: the key role of regeneration dynamics. *Glob. Planet. Chang.* 144, 94–108.
- Martinez-Vilalta, J., Poyatos, R., Aguade, D., Retana, J., Mencuccini, M., 2014. A new look at water transport regulation in plants. *New Phytol.* 204, 105–115.
- Martin-StPaul, N., Delzon, S., Cochard, H., 2017. Plant resistance to drought depends on timely stomatal closure. *Ecol. Lett.* 20, 1437–1447.
- Mccutchan, H., Shackel, K.A., 1992. Stem-water potential as a sensitive indicator of water stress in prune trees (*Prunus domestica* L. cv. French). *J. Am. Soc. Hortic. Sci.* 117, 607–611.
- McDowell, N., Pockman, W.T., Allen, C.D., Breshears, D.D., Cobb, N., Kolb, T., Plaut, J., Sperry, J., West, A., Williams, D.G., et al., 2008. Mechanisms of plant survival and mortality during drought: why do some plants survive while others succumb to drought? *New Phytol.* 178, 719–739.
- McDowell, N.G., Brodribb, T.J., Nardini, A., 2019. Hydraulics in the 21(st) century. *New Phytol.* 224, 537–542.
- McDowell, N.G., Allen, C.D., Anderson-Teixeira, K., Aukema, B.H., Bond-Lamberty, B., Chini, L., Clark, J.S., Dietze, M., Grossiord, C., Hanbury-Brown, A., et al., 2020. Pervasive shifts in forest dynamics in a changing world. *Science* 368, 964–.
- Meinzer, F.C., Domec, J.C., Johnson, D.M., McCulloh, K.A., Woodruff, D.R., 2013. The dynamic pipeline: homeostatic mechanisms that maintain the integrity of xylem water transport from roots to leaves. *Ix International Workshop on Sap Flow (991)*, 125–131.
- MeteoSwiss, 2016a. Monthly and Yearly Mean Temperature: TabsM and TabsY. MeteoSwiss, Zürich, CH.
- MeteoSwiss, 2016b. Monthly and Yearly Precipitation: RhiresM and RhiresY. MeteoSwiss, Zürich, CH.
- Milano, M., Reynard, E., Koplín, N., Weingartner, R., 2015. Climatic and anthropogenic changes in Western Switzerland: impacts on water stress. *Sci. Total Environ.* 536, 12–24.
- Müller, E., Stierlin, H.R., 1990. Sanasilva-Kronenbilder mit Nadel- und Blattverlustprozenten. Sanasilva Tree Crown Photos. Eidg. Forschungsanstalt für Wald, Schnee und Landschaft WSL, Birmensdorf, CH.
- Nahm, M., Matzarakis, A., Rennenberg, H., Gessler, A., 2007. Seasonal courses of key parameters of nitrogen, carbon and water balance in European beech (*Fagus sylvatica* L.) grown on four different study sites along a European North-South climate gradient during the 2003 drought. *Trees-Structure and Function* 21, 79–92.
- Nardini, A., Battistuzzo, M., Savi, T., 2013. Shoot desiccation and hydraulic failure in temperate woody angiosperms during an extreme summer drought. *New Phytol.* 200, 322–329.
- Nardini, A., Casolo, V., Dal Borgo, A., Savi, T., Stenni, B., Bertocin, P., Zini, L., McDowell, N.G., 2016. Rooting depth, water relations and non-structural carbohydrate dynamics in three woody angiosperms differentially affected by an extreme summer drought. *Plant Cell and Environment* 39, 618–627.
- Oliveira, R.S., Christoffersen, B.O., Barros, F.D., Teodoro, G.S., Bittencourt, P., Brum, M.M., Viani, R.A.G., 2014. Changing precipitation regimes and the water and carbon economies of trees. *Theoretical and Experimental Plant Physiology* 26, 65–82.
- Peiffer, M., Bréda, N., Badeau, V., Granier, A., 2014. Disturbances in European beech water relation during an extreme drought. *Ann. For. Sci.* 71, 821–829.
- Peuke, A.D., Gessler, A., Rennenberg, H., 2006. The effect of drought on C and N stable isotopes in different fractions of leaves, stems and roots of sensitive and tolerant beech ecotypes. *Plant Cell and Environment* 29, 823–835.
- Pflug, E.E., Buchmann, N., Siegwolf, R.T.W., Schaub, M., Rigling, A., Arend, M., 2018. Resilient leaf physiological response of European beech (*Fagus sylvatica* L.) to summer drought and drought release. *Front. Plant Sci.* 9.
- Phillips, R.P., Ibanez, I., D'Orangeville, L., Hanson, P.J., Ryan, M.G., McDowell, N.G., 2016. A belowground perspective on the drought sensitivity of forests: towards improved understanding and simulation. *For. Ecol. Manag.* 380, 309–320.
- Piedallu, C., Gegout, J.C., Bruand, A., Seynave, I., 2011. Mapping soil water holding capacity over large areas to predict potential production of forest stands. *Geoderma* 160, 355–366.
- Piedallu, C., Cheret, V., Denux, J.P., Perez, V., Azcona, J.S., Seynave, I., Gegout, J.C., 2019. Soil and climate differently impact NDVI patterns according to the season and the stand type. *Sci. Total Environ.* 651, 2874–2885.
- Poyatos, R., Aguade, D., Martinez-Vilalta, J., 2018. Below-ground hydraulic constraints during drought-induced decline in Scots pine. *Ann. For. Sci.* 75.
- R Core Team, 2019. R: A Language and Environment for Statistical Computing. R Development Core Team, Vienna, AT.
- Rambal, S., 1984. Water balance and pattern of root water uptake by a *Quercus Coccifera* L. evergreen scrub. *Oecologia* 62, 18–25.
- Remund, J., Rihm, B., Huguenin-Landl, B., 2014. Klimadaten für die Waldmodellierung für das 20. und 21. Jahrhundert. Eidg. Forschungsanstalt für Wald, Schnee und Landschaft WSL, Birmensdorf, CH <https://doi.org/10.32929/ethz-a-010693673> available online.
- Rodriguez-Dominguez, C.M., Brodribb, T.J., 2020. Declining root water transport drives stomatal closure in olive under moderate water stress. *New Phytol.* 225, 126–134.
- Rood, S.B., Patino, S., Coombs, K., Tyree, M.T., 2000. Branch sacrifice: cavitation-associated drought adaptation of riparian cottonwoods. *Trees-Structure and Function* 14, 248–257.
- Ryan, M.G., Yoder, B.J., 1997. Hydraulic limits to tree height and tree growth. *Bioscience* 47, 235–242.
- Scherrer, D., Bader, M.K.F., Körner, C., 2011. Drought-sensitivity ranking of deciduous tree species based on thermal imaging of forest canopies. *Agric. For. Meteorol.* 151, 1632–1640.
- Schleppi, P., Thimonier, A., Walthert, L., 2011. Estimating leaf area index of mature temperate forests using regressions on site and vegetation data. *For. Ecol. Manag.* 261, 601–610.
- Schuld, B., Knutzen, F., Delzon, S., Jansen, S., Muller-Haubold, H., Burlett, R., Clough, Y., Leuschner, C., 2016. How adaptable is the hydraulic system of European beech in the face of climate change-related precipitation reduction? *New Phytol.* 210, 443–458.
- Schuld, B., Buras, A., Arend, M., Vitasse, Y., Beierkuhnlein, C., Damm, A., Gharun, M., Grams, T.E.E., Hauck, M., Hajek, P., et al., 2020. A first assessment of the impact of the extreme 2018 summer drought on Central European forests. *Basic and Applied Ecology* 45, 86–103.

- Sitková, Z., Nalevanková, P., Střelcová, K., Fleischer, P.J., Ježík, M., Sitko, R., Pavlenda, P., Hlásny, T., 2014. How does soil water potential limit the seasonal dynamics of sap flow and circumference changes in European beech? *Lesn. Cas. For. J.* 60, 19–30.
- Sperry, J.S., 2000. Hydraulic constraints on plant gas exchange. *Agric. For. Meteorol.* 104, 13–23.
- Sperry, J.S., Love, D.M., 2015. What plant hydraulics can tell us about responses to climate-change droughts. *New Phytol.* 207, 14–27.
- Sperry, J.S., Donnelly, J.R., Tyree, M.T., 1988. A method for measuring hydraulic conductivity and embolism in xylem. *Plant Cell and Environment* 11, 35–40.
- Sperry, J.S., Stiller, V., Hacke, U.G., 2002. Soil water uptake and water transport through root systems. In: Waisel, Y., Eshel, A., Kafkafi, U. (Eds.), *Plant Roots. The Hidden Half*. Marcel Dekker, Inc, New York, USA, pp. 663–681.
- Stojnic, S., Suchocka, M., Benito-Garzon, M., Torres-Ruiz, J.M., Cochard, H., Bolte, A., Cocozza, C., Cvjetkovic, B., de Luis, M., Martinez-Vilalta, J., et al., 2018. Variation in xylem vulnerability to embolism in European beech from geographically marginal populations. *Tree Physiol.* 38, 173–185.
- Taiz, L., Zeiger, E., 2010. *Plant Physiology*. Sinauer Associates Inc, Sunderland, MA, USA.
- Teepe, R., Dilling, H., Beese, F., 2003. Estimating water retention curves of forest soils from soil texture and bulk density. *J. Plant Nutr. Soil Sci.* 166, 111–119.
- Thimonier, A., Sedivy, I., Schleppei, P., 2010. Estimating leaf area index in different types of mature forest stands in Switzerland: a comparison of methods. *Eur. J. For. Res.* 129, 543–562.
- Trenberth, K.E., Dai, A.G., van der Schrier, G., Jones, P.D., Barichivich, J., Briffa, K.R., Sheffield, J., 2014. Global warming and changes in drought. *Nat. Clim. Chang.* 4, 17–22.
- Trueba, S., Pan, R.H., Scoffoni, C., John, G.P., Davis, S.D., Sack, L., 2019. Thresholds for leaf damage due to dehydration: declines of hydraulic function, stomatal conductance and cellular integrity precede those for photochemistry. *New Phytol.* 223, 134–149.
- Tyree, M.T., Sperry, J.S., 1989. Vulnerability of xylem to cavitation and embolism. *Annu. Rev. Plant Physiol. Plant Mol. Biol.* 40, 19–38.
- Tyree, M.T., Cochard, H., Cruziat, P., Sinclair, B., Ameglio, T., 1993. Drought-induced leaf shedding in walnut - evidence for vulnerability segmentation. *Plant Cell and Environment* 16, 879–882.
- Urli, M., Porte, A.J., Cochard, H., Guengant, Y., Burrell, R., Delzon, S., 2013. Xylem embolism threshold for catastrophic hydraulic failure in angiosperm trees. *Tree Physiol.* 33, 672–683.
- Vanhellemont, M., Sousa-Silva, R., Maes, S.L., Van den Bulcke, J., Hertzog, L., De Groote, S.R.E., Van Acker, J., Bonte, D., Martel, A., Lens, L., et al., 2019. Distinct growth responses to drought for oak and beech in temperate mixed forests. *Sci. Total Environ.* 650, 3017–3026.
- Walthert, L., Meier, E.S., 2017. Tree species distribution in temperate forests is more influenced by soil than by climate. *Ecology and Evolution* 7, 9473–9484.
- Walthert, L., Schleppei, P., 2018. Equations to compensate for the temperature effect on readings from dielectric Decagon MPS-2 and MPS-6 water potential sensors in soils. *J. Plant Nutr. Soil Sci.* 181, 749–759.
- Warren, J.M., Meinzer, F.C., Brooks, J.R., Domec, J.C., 2005. Vertical stratification of soil water storage and release dynamics in Pacific Northwest coniferous forests. *Agric. For. Meteorol.* 130, 39–58.
- Wason, J.W., Anstreicher, K.S., Stephansky, N., Huggett, B.A., Brodersen, C.R., 2018. Hydraulic safety margins and air-seeding thresholds in roots, trunks, branches and petioles of four northern hardwood trees. *New Phytol.* 219, 77–88.
- Weber, P., Bugmann, H., Pluess, A.R., Walthert, L., Rigling, A., 2013. Drought response and changing mean sensitivity of European beech close to the dry distribution limit. *Trees* 27, 171–181.
- Wheeler, J.K., Huggett, B.A., Tofte, A.N., Rockwell, F.E., Holbrook, N.M., 2013. Cutting xylem under tension or supersaturated with gas can generate PLC and the appearance of rapid recovery from embolism. *Plant Cell and Environment* 36, 1938–1949.
- Williams, A.P., Allen, C.D., Macalady, A.K., Griffin, D., Woodhouse, C.A., Meko, D.M., Swetnam, T.W., Rauscher, S.A., Seager, R., Crissino-Mayer, H.D., et al., 2013. Temperature as a potent driver of regional forest drought stress and tree mortality. *Nat. Clim. Chang.* 3, 292–297.
- Wolfe, B.T., Sperry, J.S., Kursar, T.A., 2016. Does leaf shedding protect stems from cavitation during seasonal droughts? A test of the hydraulic fuse hypothesis. *New Phytol.* 212, 1007–1018.
- Zweifel, R., Zeugin, F., 2008. Ultrasonic acoustic emissions in drought-stressed trees - more than signals from cavitation? *New Phytol.* 179, 1070–1079.
- Zweifel, R., Zimmermann, L., Newbery, D.M., 2005. Modeling tree water deficit from microclimate: an approach to quantifying drought stress. *Tree Physiol.* 25, 147–156.
- Zweifel, R., Haeni, M., Buchmann, N., Eugster, W., 2016. Are trees able to grow in periods of stem shrinkage? *New Phytol.* 211, 839–849.